M 2015

U.PORTO
FEUP FACULDADE DE ENGENHARIA
UNIVERSIDADE DO PORTO

DEVELOPMENT OF AN INJECTABLE MODIFIED CALCIUM PHOSPHATE (BONELIKE)-DEXTRIN HYDROGEL BIOMATERIAL FOR BONE REGENERATION

ANTERO JESUS DA SILVA OLIVEIRA

DISSERTAÇÃO DE MESTRADO APRESENTADA
À FACULDADE DE ENGENHARIA DA UNIVERSIDADE DO PORTO EM
MESTRADO EM ENGENHARIA BIOMÉDICA

U.PORTO
FEUP FACULDADE DE ENGENHARIA UNIVERSIDADE DO PORTO

MEB - MESTRADO EM ENGENHARIA BIOMÉDICA | **2014/2015**

A Dissertação intitulada

"Development of an injectable modified calcium phosphate (Bonelike)-dextrin hydrogel biomaterial for bone regeneration"

foi aprovada em provas realizadas em 15-07-2015

o júri

Presidente Professor Doutor João Manuel Ribeiro da Silva Tavares
Professor Associado c/ Agregação do Departamento de Engenharia Mecânica da Faculdade de Engenharia da U. Porto

Professora Doutora Simone Barreira Morais
Professor Adjunto do Departamento de Engenharia Química da Instituto Superior de Engenharia do Porto do Instituto Politécnico do Porto

Professor Doutor José Domingos da Silva Santos
Professor Associado do Departamento de Engenharia Metalúrgica e de Materiais da Faculdade de Engenharia da U. Porto

O autor declara que a presente dissertação (ou relatório de projeto) é da sua exclusiva autoria e foi escrita sem qualquer apoio externo não explicitamente autorizado. Os resultados, ideias, parágrafos, ou outros extratos tomados de ou inspirados em trabalhos de outros autores, e demais referências bibliográficas usadas, são corretamente citados.

Autor - Antero Jesus da Silva Oliveira

Faculdade de Engenharia da Universidade do Porto

Faculty of Engineering of the University of Porto

Development of an injectable modified calcium phosphate (Bonelike)-dextrin hydrogel biomaterial for bone regeneration

Antero Oliveira

Dissertation carried out under the
Master in Biomedical Engineering

Supervisor: Prof. Dr. José Domingos Santos
Co-supervisor: Prof. Dr. Miguel Gama

June 2015

Resumo

O desenvolvimento de biomateriais compósitos pode tirar partido de sinergias entre as propriedades benéficas de dois ou mais materiais numa nova e sofisticada matriz, uma vez que poucos biomateriais possuem todas as características necessárias para apresentarem um desempenho ideal. O osso é um exemplo perfeito de um material compósito criado pela natureza.

O principal objetivo deste estudo foi o de produzir um biomaterial compósito para a regeneração do tecido ósseo. O material desenvolvido é composto por uma hidroxiapatite reforçada com biovidro (Bonelike), que já demonstrou alta bioactividade e boa osteointegração, e um hidrogel biodegradável, feito a partir de dextrino oxidado (hidrogel oDex). O hidrogel irá funcionar como veículo injectável para os grânulos do Bonelike.

Para melhorar as características do injectável, o sistema foi estudado e modificado para actuar como um transportador de fármaco, nomeadamente de simvastatina, que tem reportado a capacidade de promover actividade osteoblástica e inibir a actividade osteoclástica. Primeiramente, o Bonelike foi testado como um transportador para a simvastatina e apresentou uma libertação lenta e gradual do fármaco. Em seguida, tirando partido das capacidades da nanotecnologia no campo da administração de fármacos, nanopartículas de dextrino foram utilizadas para melhorar a solubilização da simvastatina e controlar o seu perfil de libertação. As nanopartículas carregadas com simvastatina, sob as condições testadas, formam uma solução estável que liberta o fármaco em 24 horas, e revelaram de um modo geral boa biocompatibilidade.

O novo biomaterial injetável compósito para aplicações em regeneração óssea apresenta boas características de injectabilidade e propriedades promissoras como um veículo injectável para a simvastatina.

Abstract

Given that few biomaterials possess all the required characteristics to perform ideally, the development of composite biomaterials can synergize the beneficial properties of two or more materials into an improved new matrix. Bone is a perfect example of a composite material designed by nature.

The primary purpose of this study was to produce a composite biomaterial for bone tissue regeneration. The developed material is composed by a glass reinforced hydroxyapatite (Bonelike), that have already demonstrated high bioactivity plus good osteointegration, and a biodegradable hydrogel, made from oxidized dextrin (oDex hydrogel). The oDex hydrogel will perform as an injectable carrier of the Bonelike granules.

To enhance the characteristics of the injectable, the system was studied and modified to act as a drug carrier of simvastatin, a drug that has been reported to promote osteoblastic activity and inhibit osteoclastic activity. At first, Bonelike was tested as a carrier for simvastatin and showed a slow and gradual release of the drug over 2 weeks. Then, taking advantage of nanotechnology in the drug delivery field, dextrin nanoparticles were used for improving simvastatin solubilisation and controlling its release profile. The simvastatin loaded nanoparticles, under the conditions tested, form a stable solution that release its content in a 24 hours time frame and revealed an overall good biocompatibility.

The new injectable composite biomaterial for bone regeneration present good extrusion characteristics and promising properties as an injectable carrier of simvastatin.

Acknowledgments

I want to start by thanking my supervisors, for their guidance and availability. I also wanna thanks Professor Ana Colette and all Biosckin team, especially Dina.
A very special thanks to all the people in the DEB for all the support: Catarina, Paula, Isabel, Alberto, Ana Cristina, Tânia, Karol, Ana and Alexandra.
A special thanks to my housemates, Ivana and Mara, and all my friends.
Finally, my deepest gratitude to my parents and grandparents.

Contents

Lists of figures

Lists of tables

Lists of abbreviations

ADH	Adipic acid dihydrazide
BMP	Bone morphogenetic protein
DBM	Demineralized bone matrix
DCP	Dicalcium phosphate
DexC16	Hydrophobically modified dextrin
Dex-HEMA	Dextrinhydroxyethylmethacrylate
Dex-VA	Dextrin-vinyl acrylate
DLS	Dynamic light scattering
DMEM	Dulbecco´s modified Eagle´s medium
DO	Degree of oxidation
DS	Degree of substitution
DSC16	Degree of substitution of dextrin with alkyl chains
ECM	Extracellular matrix
HAp	Hydroxyapatite
MSCs	Mesenchymal stem cells
MTT	3-(4,5-dimethylthiazol-2-yl)-2,5-diphenyltetrazolium bromide
NMR	Nuclear magnetic resonance
oDex	Oxidized dextrin
PBS	Phosphate buffered saline
PLGA	Poly(lactic-co-glycolic acid)
SIM	Simvastatin
TCP	Tricalcium phosphate
TEA	Triethylamine
TeTCP	Tetracalcium phosphate

Chapter 1
Motivation and main goals

Biomaterials degree of sophistication has increased significantly; the actual trend is towards biomaterials that are capable of perform active roles, in which they can assist and promote tissues regeneration.

Selecting an appropriate material can lead to an improvement on the quality of the newly formed tissue. The major challenge for the field of tissue engineering is the identification or development of biomaterials capable of promoting the desired outcome. Given that few biomaterials possess all the required characteristics to perform ideally, the development of hybrid or composite biomaterials can synergize the beneficial properties of two or more materials into an improved new matrix.

In this work, the development of a composite biomaterial for bone tissue regeneration was attempted. It is composed by a glass reinforced hydroxyapatite (Bonelike), that has a composition very similar to the bone mineral phase and have already demonstrated high bioactivity plus good osteointegration, and a biodegradable hydrogel, made from dextrin (oDex hydrogel), a glucose polymer with low molecular weight. The oDex hydrogel will perform as an injectable carrier of the Bonelike granules.

To enhance the characteristics of the injectable formulation, different strategies were selected and tested. The capacity of the system to act as a drug carrier of simvastatin (a cholesterol-lowering drug that recently has been reported to promote osteoblastic activity and inhibit osteoclastic activity) was tested. It is expected that simvastatin will bring osteogenic properties to the bone graft material; however, the current level of evidence regarding regenerative applications of simvastatin has not been established in a systematic way, owing to this line of research still being very recent.

Self-assembled nanoparticles are promising nanotecnhological tools with potencial in the drug delivery field. In this work, dextrin nanoparticles and Bonelike were selected as carriers for the simvastatin and a release study was performed. The cytotoxicity of the simvastatin loaded nanoparticles was also evaluated.

The injectability of the whole system was also assessed, with the view to its application in clinical environment.

Chapter 2
State of the art

2.1 Bone
2.1.1 Structure
Bone tissue is the major structural and supportive connective tissue of the body. It is a living, highly vascularized, dynamic, mineralized connective tissue that forms the skeleton of the most vertebrates [1], [2].

Bone presents a unique structure and mechanical properties: it is one of the most rigid and resistant tissue of the human body and have relatively light structure, capable of supporting considerable forces and able to remodel and repair itself. Bone is a dense multi-phase material or composite made up of cells embedded in a matrix composed of both organic and inorganic elements [1], [3], [4].

However, its structure and proportion of its components differ widely with age and site, resulting in different classifications of bone that exhibit various mechanical and functional characteristics [1].

The skeleton is designed to protect the vital organs of the body and provide the frame for locomotion of the musculoskeletal system. Furthermore, bone is a reservoir for many essential minerals, such as calcium and phosphate, and plays an important role in the regulation of the ion concentrations in extracellular fluid [5].

Bone marrow contains mesenchymal stem cells (MSCs), which are multipotent cells capable of differentiation into bone, cartilage, tendon, muscle, skin and fat tissue. In this cavity, there are also different kinds of hematopoietic cells that produce the red and white blood cells, that have the function of gas transportation and immune resistance, respectively [5], [6] .

The adult human skeleton is composed of 20% trabecular bone and 80% cortical bone (figure 2.1) [7]. In the body, different bones show different percentages of cortical and trabecular bone [8].

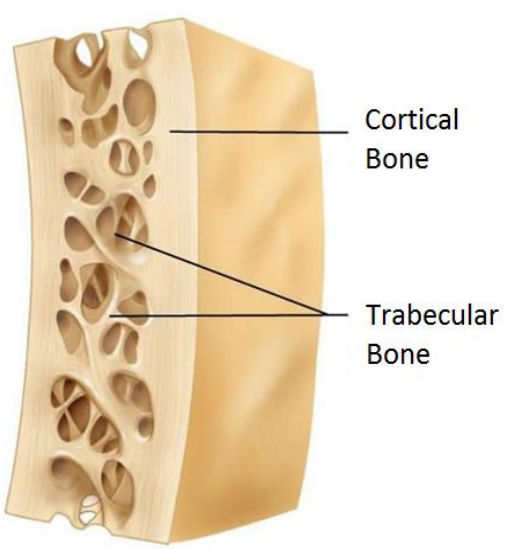

Figure 2.1 - Cortical bone and trabecular bone [7].

Cortical bone is also called compact bone or haversian bone and it is typically found in the shafts of long bone and the vertebral endplates [9]. Cortical bone has only 10% of porosity, whit a small number of cells and blood vessels. The structural unit of cortical bone is the cylindric shaped osteon, which is composed of concentric layers of bone called lamella [5], [10]. Blood vessels are present along the Haversian canals located at the center of each osteon. The nutrient diffusion is further allowed by microscale canals within the bone. Osteons are aligned in the longitudinal direction of bone and therefore, cortical bone is anisotropic [5].

Trabecular bone is also called cancellous bone and is primarily found in the vertebral bodies, pelvis, and distal ends of long bones [9]. Trabecular bone, which may has as much as 50 – 90 % pores, is an interconnected network of small bone trusses (trabecula) aligned in the direction of loading stress. The porous of cancellous bone contains vessels and bone marrow, which provides lower mechanical support compared to cortical bone [5], [9].

2.1.2 Extracellular matrix and bone cells

Bone tissue is essentially constituted of an extracellular matrix and three main cell types. The extracellular matrix is a composite of inorganic (65%) and organic (35%) phases. Calcium-containing minerals are the components of the inorganic part. The organic part of the extracellular matrix is composed of collagen type I and numerous noncollagenous proteins, like bone sialoprotein, osteocalcin and osteopontin [11]. This organic matrix is calcified by the deposition of crystals of the mineral phase, which is a highly substituted hydroxyapatite [12]–[14].

Three types of differentiated cells inhabit the organic-inorganic composite structure of bone. These cells are osteoblasts, osteoclasts and osteocytes [5], [15], [16].
The osteoblasts are fully differentiated cells responsible for the production of the extracellular bone matrix and its mineralization and they also manufacture hormones, such as prostaglandins, to act on bone itself. They produce alkaline phosphatase, an enzyme that has a role in bone mineralization. Osteoblasts originates from less differentiated precursor cells known as osteoprogenitor or MSCs [16]–[18].

Osteocytes are the most abundant cell type in bone. They are responsible for bone matrix maintenance by secreting enzymes and maintaining its mineral content. The osteocytes derive from osteoblasts and they are not on the bone surface but regularly entrapped throughout the extracellular matrix [16], [17].
Osteoclasts are giant multinucleated cells responsible for bone resorption. Unlike osteoblastic cells, osteoclasts are derived from hematopoietic cell lines of macrophage/monocyte linage. Osteoclasts differentiation occurs within the bone microenvironment, where interaction between monocyte precursors and osteoblasts enables the cells to differentiate into osteoclasts [16], [17], [19].

2.1.3 Bone remodeling and repair

Bone is a living organ that undergoes remodelling throughout life. Bone remodeling is an active and dynamic process that relies on the correct balance between bone resorption by osteoclasts and bone deposition by osteoblasts (figure 2.2) [20], [21]. Bone remodeling involves the removal of mineralized bone by osteoclasts followed by the formation of bone matrix through the osteoblasts that subsequently become mineralized. The remodeling cycle consists of three consecutive phases: resorption, during which osteoclasts digest old bone; reversal, when mononuclear cells appear on the bone surface; and formation, when osteoblasts lay down new bone until the resorbed bone is completely replaced [19].

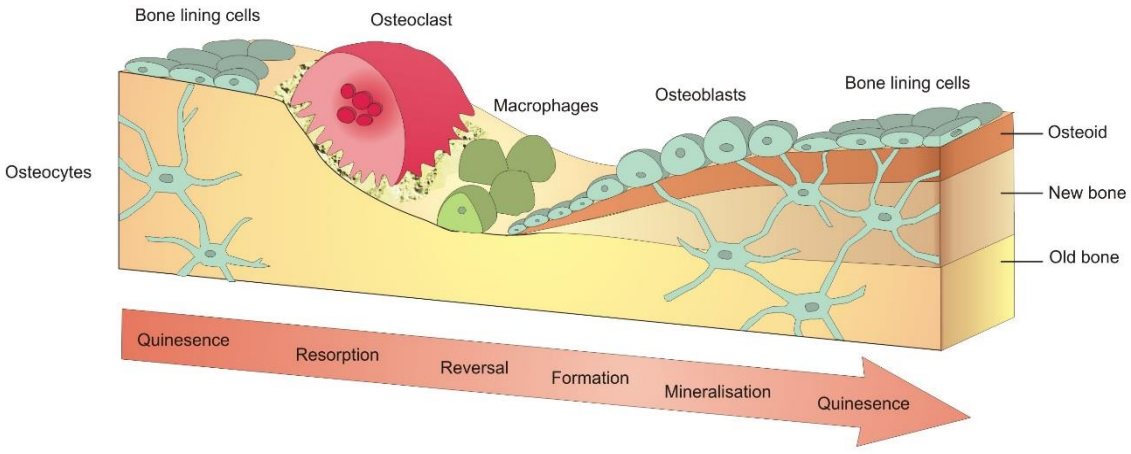

Figure 2.2 - Bone remodeling process [21].

Moreover, these functions must be tightly coupled not only quantitatively, but also in time and space. When the coupling is lost, the correct bone mass could be compromised, leading to several skeletal pathologies [20].
The process of fracture healing can be considered a form of tissue regeneration. However, despite the regenerative capacity of skeletal tissue, this biological process sometimes fails and fractures may heal in unfavourable anatomical positions, show a delay in healing or even develop pseudoarthrosis or non-unions [22], [23].

Healing occurs in three distinct but overlapping stages: the early inflammatory stage; the repair stage; and the late remodeling stage (figure 2.3) [23], [24].

In the inflammatory stage, a hematoma develops within the fracture site during the first few hours and days. Inflammatory cells (macrophages, monocytes, lymphocytes, and polymorphonuclear cells) and fibroblasts infiltrate the bone under prostaglandin mediation. This results in the formation of granulation tissue, ingrowth of vascular tissue, and migration of mesenchymal cells. The primary nutrient and oxygen supply of this early process is provided by the exposed cancellous bone and muscle [25], [26].

During the repair stage, fibroblasts begin to lay down a stroma that helps support vascular ingrowth. With the progress of the vascular ingrowth, a collagen matrix is laid down while osteoid is secreted and subsequently mineralized, which leads to the formation of a soft callus around the repair site. This callus is very weak, in terms of resistance to movement, during the first 4 to 6 weeks of the healing process and usually requires adequate protection in the form of bracing or internal fixation, being these events related to the orthopaedic area. Eventually, the callus ossifies, forming a bridge of woven bone between the fracture fragments. Otherwise, if proper immobilization is not applied, ossification of the callus may not occur, and an unstable fibrous union may develop instead [23], [25]. Fracture healing is completed during the remodeling stage in which the healing bone is restored to its original shape, structure, and mechanical strength [19], [25].

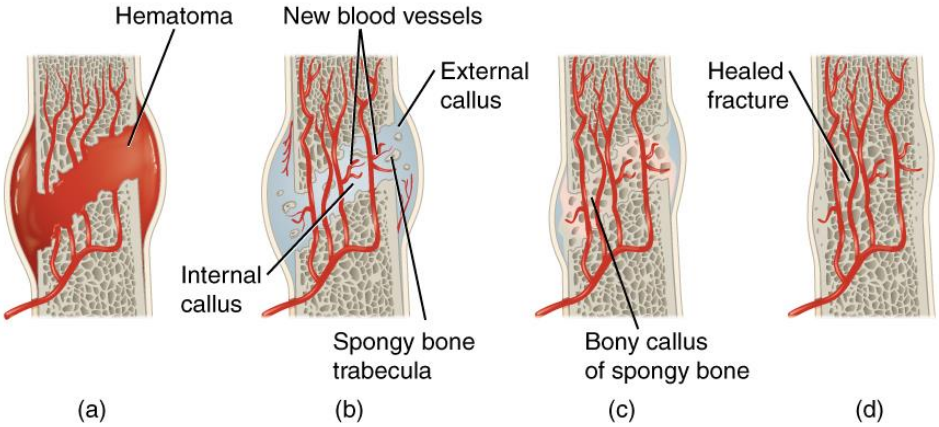

Figure 2.3 - Process of fracture healing: (a) inflammation, (b) soft callus, (c) hard callus and (d) remodelling [24].

2.2 Bone grafts

2.2.1 Introduction

The field of biomaterials incorporates a broad spectrum of ideas, sciences and technologies, and it is in constant evolution. The applications of materials to problems in biology and medicine requires follow the medical needs and the technological advance and research, always considering the ethical concerns and implications [27].

Advances in engineering - for example nanotechnology - are greatly increasing the sophistication with which biomaterials are designed and have allowed fabrication of materials with increasingly complex functions [28].

Biomaterials are widely used to replace and/or restore the function of traumatized or degenerated tissues or organs, and thus improve the quality of life of the patients. The first and foremost requirement for the choice of the biomaterial is its acceptability by the human body. The most common classes of materials used as biomedical materials are metals, polymers, ceramics, and composite. These four classes are used singly and in combination to form most of the implantation devices available today [29].

2.2.2 Bone grafts

Autograft bone is the bone of a patient for use in grafting procedures in their own body. Bone is taken from one part of the body and grafted onto another to replace damaged tissues (figure 2.4). This procedure present a high probability of successful bone fusion, non-rejection and absence of transition of diseases [30]. Despite having osteogenic, osteoinductive and osteoconductive properties, autograft procedure involves a second surgery to harvest the bone graft and could result in additional chronic pain at the site where the bone was harvested [31]. Besides that, the quantities of autograft bone are limited and the mortality of the tissue related with the harvesting is around 10% [30].

An allograft is a graft between genetically non-identical members of the same specie. An allograft may be obtained from living donors who are having bone removed during surgery or cadaveric ones. In these cases, there are no limitations with the volume of available tissue, and it is not necessary a second surgery in the patient [32]. It is possible to obtain a different variety of physical forms, like powder, gel, fibers, pastes, etc [33]. The major disadvantage of this graft is the transmission of diseases. Due to processing and sterilization, the graft loses the osteogenic capacity and presents the possibility of rejection [33]–[35].

Xenograft bone substitute has its origin from a species other than human, such as bovine bone and porcine bone and, more recently, coral [36]. However it is necessary several treatments such antigenic, demineralization and deproteinization, resulting in a loss of osteoinductive capacity [37]. The principal advantage is the large amount of available material; however, the risk of viral and bacterial diseases still occurs [38].

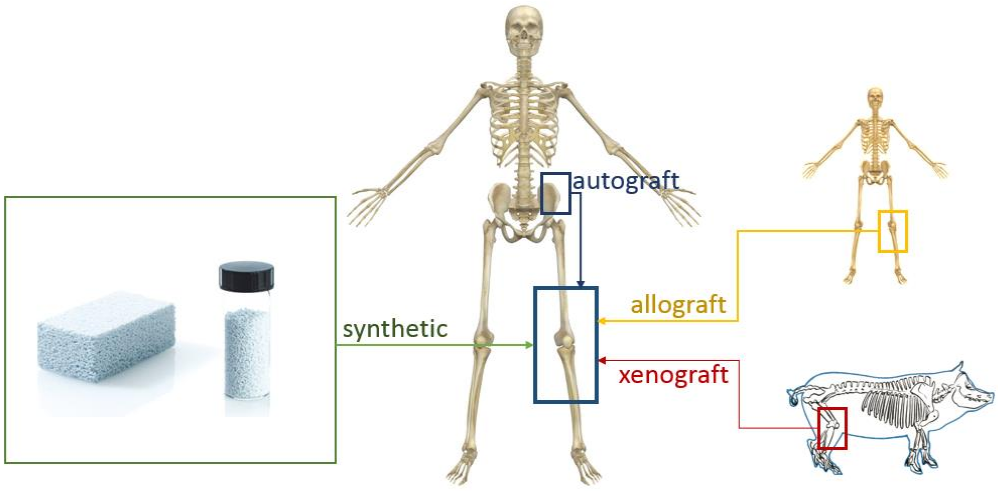

Figure 2.4 - Various types of bone graft sources.

Although autograft is still perceived as the gold-standard material in bone grafting, the wide array of alternatives available in the market has resulted in a gradual shift towards increased adoption of bone grafts and substitutes, especially in the US and European market. The global bone grafts and substitutes market value will increase steadily over the coming years, rising from almost $2.1 billion in 2013 to approximately $2.7 billion by 2020, at a Compound Annual Growth Rate of 3.8% [39].

2.2.3 Synthetic materials

2.2.3.1 Calcium phosphate-based materials

Due to their abundance in nature and presence in living organisms, calcium apatites and other calcium orthophosphates remain the chemical compounds of a special interest in many fields of science, including geology, chemistry, biology and medicine [40]–[42]. Synthetic materials, such as calcium phosphate ceramics (e.g. hydroxyapatite ($Ca_{10}(PO_4)_6(OH)_2$, HAp), tricalcium phosphate ($Ca_3(PO_4)_2$, TCP), dicalcium phosphate ($Ca_2P_2O_7$, DCP) and tetracalcium phosphate ($Ca_4P_2O_9$, TeCP), etc.) are graft materials used in the bone tissue regenerative process [38], [43]–[45].

Successful bone grafting has to follow four basic criteria: osteoinduction, osteoconduction, osteogenesis, and stability [30]. Osteoinduction refers to the stimulation of osteoprogenitor cells to differentiate into osteoblasts that then begin new bone formation. Osteoconduction is the process which provides a structural framework and environment that supports the migration, attachment and growth of osteoblasts and osteoprogenitor cells into the graft. Osteogenesis refers to cellular process of new bone formation by osteoblasts following osteoinduction [46]. Finally, stability, or movement resistance ability at the union site, is crucial to avoid delayed neovascularisation, which could result in an inadequate growth of the newly formed bone over the bone graft leading to pseudoarthrosis [30], [38], [43], [47].

Calcium phosphate-based materials are of great interest for use as bone synthetic graft materials due to their chemical and biological properties, similar to human bone [43], [47]. These graft materials do not possess the risk of disease transmission and eliminate the need for an additional surgical procedure for transplantation, reducing patient pain and recovery time [38], [47]. In regenerative medicine, bone graft to restore skeletal integrity, give mechanical support and enhance bone healing is used in several orthopaedic, dental and maxillofacial procedures[48]–[54].

2.2.3.2 Bioactive glasses and glass-ceramics

Bioactive glasses are amorphous materials and glasses ceramics are polycrystalline materials composed of one or more glassy and crystalline phases. For the preparation of glass-ceramic materials there are three main techniques used: casting and controlled crystallization; sintering and crystallization of glass powder; and sol-gel technique [55]–[57].

Almost all of the bioactive glasses and glass-ceramics currently used contain large amounts of silica (SiO_2). Specific additives may be incorporated into the base glass composition to induce the nucleation and growth of particular crystal phases, within the residual vitreous matrix, with specific physicochemical properties in order to obtain glass-ceramics. The characteristics of

the final constituent phases and microstructure of the glass-ceramic establish its properties and main applications. The most well-known glass-based materials are Bioglass®, Ceravital® and Cerabone® A/W [58]–[60]. Several clinical applications of bioactive glasses and glass ceramics are reported in the literature [61]–[66].

All materials elicit a response from the host when implanted in living tissues. Generally, both tissue and material undergo physical and/or chemical modifications. Based on these modifications, ceramics can be classified as nearly inert ceramics, surface reactive ceramics (bioactive) and bioresorbable ceramics [67]–[69]. The nearly inert ceramics such as alumina and carbons are chemically stable and elicit minimal response within the surrounding tissue, maintaining its characteristics throughout the entire period of implantation in the organism [27], [70], [71].

The surface reactive ceramics are midway between nearly inert and resorbable in behaviour. This kind of ceramic elicits a biological response to facilitate a direct chemical bond between the material surface and the surrounding tissues. The glass-based materials are considered surface reactive ceramics and some examples included in this group are bioactive glasses (Bioglass®) and glass-ceramics (Ceravital®, Cerabone A/W)[27], [58], [70], [72]. When implanted, the materials undergo dissolution and release ions into the surrounding environment with consequent local pH changes. The composition of the materials controls their surface reactivity. These kinds of materials do not become encapsulated when implanted, but closely adhere to the surrounding living bone tissues. The glass, glass-ceramics and calcium phosphates that show the ability to bond to bone after implantation became known as bioactive ceramics [73], [74].

Bioresorbable ceramics are designed to degrade progressively with time and be replaced with natural host tissue, without toxicity and rejection. Bioresorbable materials may show some complications in the clinical use, such as maintenance of strength and stability, and matching resorption rates to the repair rates of body tissues. This point is very important, since some materials display precocious resorption or delayed resorption. Since a great concentration of ions or/and particles of a bioresorbable material is released, it is important that it consists only of metabolically tolerable substances, which restricts the material's compositional design and therefore the mechanical behaviour and eventually its final applications [27], [68], [75], [76].

2.2.3.3 Glass reinforced apatite

A synthetic hydroxyapatite sintered in the presence of $CaO\text{-}P_2O_5$ based glasses, forms a material patented as Bonelike®, that was designed to improve the mechanical properties of calcium phosphate ceramics and mimic the inorganic composition of bone tissue [49], [52], [77], [78].

Its composition has the advantage of mimicking the mineral composition of natural bone. In fact, the addition of $CaO\text{-}P_2O_5$ based glass into the HAp structure leads to the formation of secondary phases, α- and ß-TCP. Their percentage is dependent upon the sintering treatment, content and the composition of the glass added. Due to the presence of α- and ß-TCP in the HAp matrix of Bonelike® the mechanical properties of the material are improved. Furthermore, this biodegradable and bioresorbable phases allow a local enrichment in calcium, phosphorous and several ionic species, such as magnesium, sodium and fluoride, that in physiological conditions uphold a positive effect in the biomaterial's behaviour since they promote osteointegration and enhance bone regeneration [79], [80].

Clinical applications of Bonelike® in maxillofacial surgery indicate perfect bone bonding between new bone formed and Bonelike granules, along with partial surface biodegradation. This quick and effective osteoconductive response from Bonelike reduce the time needed to reconstruct the bone defected area of patients [50], [81] .

The controlled biodegradation of Bonelike® strongly enhances new bone formation and stimulates the revascularization of the bone tissue. A clinical report were Bonelike® was implanted in eleven patients, to repairing surgical cystic bone defects, showed that after 48 weeks of implantation all the patients showed high bone regeneration and none of the patients presented any symptoms of rejection or infection [81].

2.2.4 Injectable bone graft substitutes

Injectable bone substitutes that are self-setting *in situ* can bring substantial benefits in some clinical situations, such as augmentation of osteoporotic fractures, treatment of maxillofacial defects and deformities. In fact, the orthopaedic community is still within the learning curve in many aspects of many of these products since they were introduced to the market not long ago [82], [83].

Most injectable bone substitutes consist of a powder and a liquid or gel that are mixed immediately before use [82], [83]. The ability of the surgeon to properly mix and inject the material within the prescribed time is crucial. In addition, the force needed to extrude the material should be taken into consideration.
In table 2.1, a research was made to quantify some of the injectable bone graft substitutes that were commercially available in 2014. The Food and Drug Administration (FDA) approved all products presented in the table [83], [84].

Table 2.1 - Injectable bone grafts commercially available

Company	Commercially available product	Composition
AlloSource	AlloFuse	Heat sensitive copolymer with DBM
Biomet Osteobiologics	InterGro	DBM in a lecithin carrier
Exactech	Optecure	DBM suspended in a hydrogel carrier
	Optefil	DBM suspended in a gelatin carrier
Integra Orthobiologics	Accell Evo 3	DBM, Accel Bone Matrix and Reverse Phase Medium
	DynaGraft II	DBM and Reverse Phase Medium
	OrthoBlast II	DBM, cancellous bone and Reverse Phase Medium
Life Net Health	Optium DBM	DBM combined with glycerol carrier

BioHorizons	Osteofil DBM	DBM in porcine gelatin
	Progenix Putty	DBM in Type-1 bovine collagen and sodium alginate
MTF/Synthes	DBX	DBM in sodium hyaluronate carrier
Osteotech	GRAFTON gel	DBM in a syringe
Smith & Nephew	VIAGRAF	DBM combined with glycerol
Wright Medical Technology	PRO-DENSE injectable Regenerative Graft	75% calcium sulphate and 25% calcium phosphate

The polymers used as carriers must have rheological, mechanical and biological properties appropriate to its applications and the site of the implant [83], [85], [86]. Possible toxicity of degradation products and their elimination routes also need to be considered [85]. These injectable systems should allow minimally invasive implantation, fill a desired shape, and easy incorporation of various therapeutic agents [85].
In fact, one of the most attractive features of injectable bone substitutes, besides providing mechanical support, is their potential use for controlled release of therapeutic or bioactive agents [87].

2.3 Hydrogels

2.3.1 Introduction

Hydrogels are water-swollen polymeric materials, with a stable three-dimensional structure that provide scaffolds for tissue engineering, wound dressings, and drug delivery systems, among other application[88]–[90].
Depending on their method of preparation, ionic charge, or physical structure features, hydrogels maybe classified in several categories. Based on the method of preparation, they may be homopolymer hydrogels, copolymer hydrogels, multipolymer hydrogels, or interpenetrating polymeric hydrogels[91], [92].
Hydrogels remain as appealing candidates to tissue engineering scaffolds, due to the controllable and reproducible polymer properties and to the large water uptake, promoting excellent biocompatibility due to low protein adsorption [27]. In addition, hydrogels present mechanical properties and hydrophilicity that resembles those of the extracellular matrix (ECM) of native tissue, tunable viscoelasticity, and high permeability for oxygen and essential nutrients[93]–[97]. Despite from the favorable physico-chemical and mechanical properties, the most important requirement for a hydrogel to be used in medical applications is its biocompatibility and the non-cytoxicity of its degradation products [98], [99].

Injectable hydrogels can be maintained in the liquid state before injection and harden after transplantation *in vivo*. The hydrogel allows the filling of irregular defects, decreases the risk of implant migration and minimizes surgical defect to the size of a needle. In addition, the hydrogel can be incorporated with therapeutic factors and cells[100]. Hydrogels can also be stimuli-sensitive and respond to temperature, pH, electric field, glucose and antigens, among others. This way the hydrogel can have a controlled drug release due to volume changes [101].

Hydrogels present some limitations regarding drug delivery such as the high water content and large pore sizes that frequently result in relatively rapid release. Recently, composite systems where micro or nano hydrogels are incorporated in a bulk hydrogel matrix emerge as a platform for drug delivery [102]–[104]. The micro or nano hydrogel particles can act as a drug reservoir from which release can be triggered by a suitable stimulus or simply released in a diffusion-controlled manner [104]. The major advantage relies on the improvement of the kinetic release profile of the drug, as the nanogel phase provides an additional diffusion barrier moderating or eliminating the initial burst release typically observed in hydrogel or nanogel drug delivery systems [105].

Within the large range of materials used in the development of hydrogels, polysaccharide-based materials have been referred to as promising materials, presenting appealing properties for biomedical applications[27], [92], [106], [107].

Among the numerous macromolecules that can be used for hydrogel formation, polysaccharides are advantageous compared to synthetic polymers since they are coming from renewable sources. Polysaccharides have also frequently economic advantages over synthetic materials and they are usually non-toxic, biocompatible and show a number of convenient physico-chemical properties such as viscosity, hydrophilicity and reactive groups [108]. The major disadvantages of natural polymers, when compared with synthetic ones, are the difficulty in controlling their physico-chemical properties, such as molecular weight, strength, degradation time and mechanical properties. However, there are several strategies to overcome these limitations, like the combination with other natural (e.g., collagen/glycosaminoglycans) or synthetic polymers (e.g., collagen/PLGA). This combinations, may improve the biocompatibility of the ensuing scaffolds, by reducing inflammatory response *in vivo* and improving initial cell attachment and differentiation on the material [109]–[112]. Polysaccharides, such as starch, cellulose, chitin/chitosan, alginate, carrageenan, gellan, guar gum, hyaluronic acid, pullulan, among others, have been used in the formulation of several hydrogels [113]–[121].

2.3.2 Dextrin hydrogel

Among starch-based materials, those based on dextrin are widely used in a variety of applications, since adhesives used in food to textile industries [122], peritoneal dialysis solution [123] and the cosmetic industry [124].

Dextrins are a group of low-molecular-weight carbohydrates produced by partial hydrolysis of starch, which can be accomplished by the use of acid, enzymes, or a combination of both. Dextrin is a glucose-containing saccharide polymer linked by α-1,4 D-glucose units, containing few (< 5%) α-1,6 links, having the same general formula as starch, but smaller and less complex (figure 2.5) [107], [123].

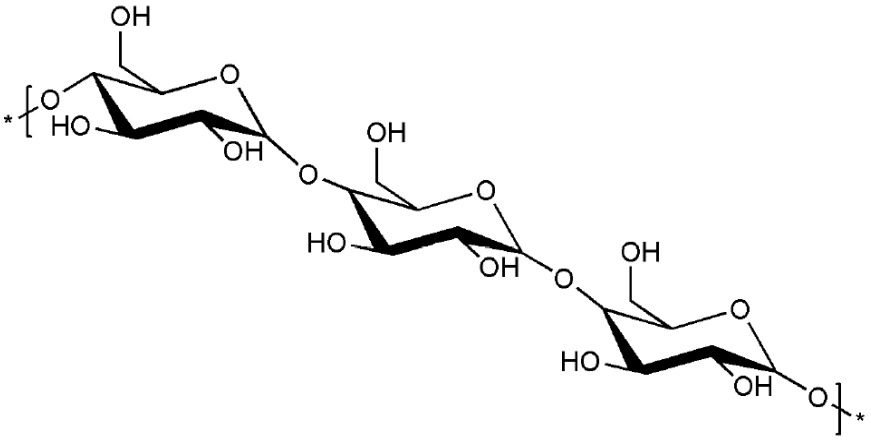

Figure 2.5 - Structure of Dextrin [125].

Due to its proven clinical tolerability [126] and its efficient absorption due to degradation by amylases [105], [127], [128], dextrin appears as a polymer that might be ideal for development as a drug carrier [123].

Dextrin hydrogels can be obtained by crosslinking following oxidation. The oxidized dextrin is characterized by their oxidation degree, which consists on the quantification of aldehyde groups. The oxidation reaction is characterized by the specific cleavage of the C2-C3 linkage of glucopyranoside rings, yielding two aldehyde groups per glucose unit (figure 2.6).

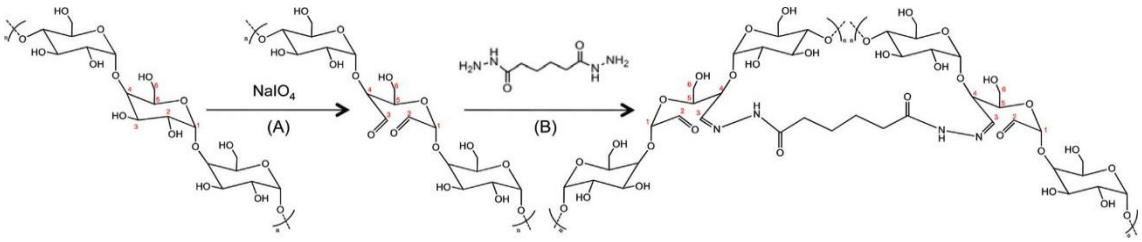

Figure 2.6 - Periodate Oxidation of Dextrin, Yielding Two Aldehyde Groups at Positions C2 and C3 of a D-Glucose Unit [105].

The degree of oxidation (DO) can be easily controlled by the relative quantity of sodium periodate used, yielding free aldehyde reactive groups to create covalent linkages with reticulating molecules, cellular adhesion binding peptides or specific drugs for controlled delivery systems [105].

In recent works, dextrin-hydroxyapatite complex was used as a bone filling material, with good performance [129]. Dextrin hydrogels, namely, dextrin-vinyl acrylate (Dex-VA) and dextrinhydroxyethylmethacrylate (Dex-HEMA) was shown their noncytotoxicity as well as their appealing diffusivity and degradability profiles for targeted delivery therapeutics [107], [130].

The concentration of dextrin that guarantees the ideal texture is between 30% and 40%, giving rise to an injectable hydrogel; above 40%, the solution is extremely viscous and very difficult

to homogenize. A polymer concentration below 25% will originate a viscous fluid instead of a hydrogel. The crosslinking times of the hydrogel is between 5-30 minutes. If used in maxillofacial surgery applications, as an adjuvant to osteogenic granular compounds, this time would allow an unhurried handling and implantation [107], [125].

2.3.3 Dextrin nanogel

Polymeric nanogels, also referred to as hydrogel nanoparticles, macromolecular micelles or polymeric nanoparticles, are emerging as promising drug carriers for therapeutic applications [131].

The study of nanogels has intensified during the past two decades due to enormous potential applications in the development and implementation of new environmentally responsive materials, biomimetics, biosensors, artificial muscles and drug delivery systems [132]. Solid nanoparticles made from biodegradable polymers for long-term delivery of drugs can potentially provide benefits such as increased therapeutic effect, prolonged bioactivity, controlled release rate, and finally decreased administration frequency, thereby increasing patient compliance [133].

Among the available nanosystems, self-assembled polymeric nanogels, like dextrin nanogel, are particularly attractive, since they are easy to produce, affordable and may effectively incorporate a variety of drugs [132].

Gonçalves *et al*. developed and characterized self-assembled nanoparticles of dextrin with great potential for biomedical applications [131], [134]–[138]. *In vitro* studies with bone marrow-derived macrophage revealed that the nanoparticles are non-cytotoxic and do not elicit a reactive response when in contact with macrophages [136]. Dextrin nanoparticles served as an effective nanocarrier for the formulation of lipophilic curcumin by increasing its water solubility, improving its stability, and controlling its release profile, without compromising the cytotoxicity in HeLa cell line [138].

2.4 Simvastatin in bone regeneration

Currently, researchers are searching for bone graft materials with the advantages of autologous bone grafts (osteogenesis, osteoinduction and osteoconduction), but without their disadvantages (donor site morbidity, difficulty of storage and maintenance, unlimited availability, etc.) [139].

In 1980, Urist reported the identification in the rat organic bone matrix of an insoluble protein of low molecular weight called Bone Morphogenetic Protein, BMP [140]. BMPs are multi-functional growth factors that belong to the transforming growth factor beta (TGFbeta) superfamily [141]. BMP signaling plays critical roles in heart, neural and cartilage development and play an important role in postnatal bone formation. Preclinical and clinical studies have shown that BMP-2 can be utilized in various therapeutic interventions such as bone defects, non-union fractures, spinal fusion, osteoporosis and root canal surgery [141]. BMP-2 and BMP-7 are osteoinductive BMPs: they have been demonstrated to potently induce osteoblast differentiation in a variety of cell types [141], [142]. However, the use of BMPs entails some problems such as

their short life, storage and handling difficulties, inefficiency in the recognition of target cells, and high cost, which has hindered its popularization in procedures for regeneration of bone tissue [139], [143].
As alternatives of BMPs, some authors have suggested the topical use of drug compounds aimed at upregulating intrinsic bone growth factors. For example, some widely known pharmacologic compounds (such as bisphosphonates or statins) have recently been shown to upregulate bone growth through distinct and complex biochemical pathways [144]–[147].
In 1999, was first reported, by Mundy *et al.*, that lovastatin and simvastatin stimulate bone regeneration when injected subcutaneously in mouse calvaria [148]. Statin is a specific inhibitor of 3-hydroxy-3-methyl-glutaryl coenzyme A (HMG-CoA) reductase, rate-limiting enzyme of the cholesterol synthesis pathway [149]. Simvastatin (figure 2.7) [150], a chemical modification of lovastatin, is an inactive lactone drug that, after oral administration, is converted to its active dihydroxy open acid form by the intracellular enzyme cytochorome P450 (3A4 isozyme) in the liver [149]. Simvastatin is not well absorbed, and less than 5% of an oral dose reaches the systemic circulation. Concentrations of statins in bone marrow have not been well established yet, but osteoblasts and osteoclasts may be exposed to very low concentrations of statin with existing oral regimens [151].

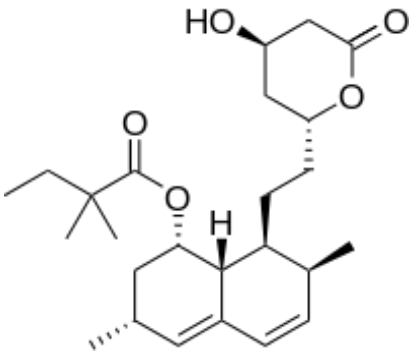

Figure 2.7 – Structure of simvastatin [150].

Simvastatin is suggested to support bone morphogenetic protein (BMP)-induced osteoblast differentiation through antagonizing TNF-α-to-Ras/Rho/mitogen activated protein kinase and augmenting BMP-Smad signalling [152]. Simvastatin increases alkaline phosphatase activity and mineralization, as well as increases the expression of bone sialoprotein, osteocalcin and type I collagen, and it is shown to have anti-inflammatory effect by decreasing the production of interleukin-6 and interleukin-8 [153].

Simvastatin has been reported to promote osteoblastic activity and inhibit osteoclastic activity. There have been many studies demonstrating the bone promoting effect of local application with different carriers in various animal models [154]–[156].
The use of topical simvastatin for bone regeneration can be seen as a relatively recent research line, since most studies have been carried out in the last 5 years [139].
The successful use of simvastatin to promote bone formation *in vivo* depends on the local concentration [154]. Therefore, an appropriate carrier would bring several advantages, including localization and retention of the molecule to the site of application thus reducing the loading dose and providing a matrix for mesenchymal cell infiltration and a substrate for cell growth

and differentiation [157]. In addition, the optimal carrier should help to define the shape of resulting new bone and should have a degradation rate that does not inhibit bone growth and prevent fibrous tissue formation or fibrous encapsulation of the carrier. There have been many studies demonstrating the osteopromotive effect achieved by the local application of the drug (table 2.2) with different carriers in various animal models [157].

Table 2.2 - Carriers and animal models used for the local application of simvastatin.

Type of carrier	Animal model	Defect	Reference
Methylcellulose gel	Miniature pigs	Alveolar defects	[146]
Polylactic acid/ polyglycolic acid	Wistar rats	Extraction sockets in mandibular incisors	[154]
Gelatin	Wistar rats	Bone defect in mandible	[155]
Methylcellulose gel	Beagle dogs	Periodontal defects	[158]
Calcium sulphate	Rabbits	Ulnar defects	[159]
α-TCP	Wistar rats	Calvarial defects	[160]

Pradeep *et al.* has carried out randomized clinical trials demonstrating that locally- administered simvastatin, versus placebo, significantly improves the clinical outcomes of scaling and root planning for treating mandibular buccal Class II furcation defects [161] and in patients with chronic periodontitis [162].
Studies focusing on pharmacological development have tested several biodegradable polymeric formulas for the local delivery of simvastatin such as a hydrogel of gelatin [163] or microspheres of PLGA [164].
The large majority of animal studies reported favorable results concerning topical application of simvastatin, either injected alone [165] or in combination with biomaterials [166], or covering acellular scaffolds [167]. Ozeç *et al.*, make a 3 mm diameter defect in the angulus mandibular region of Wista albino rats and grafted with simvastatin gelatin sponge producing 240% more new bone than the control group [155] . Nyan *et al.*, create critical-sized bone defects in rat calvaria and treated with calcium sulfate or with combination of 1 mg simvastatin and calcium sulfate. It was reported that the combination of simvastatin and calcium sulfate stimulated bone regeneration [156].

Most animal studies performed intraorally have reported good results for topical simvastatin administration in enhancing bone regeneration in rat mandibular defects [168] and periodontal lesions in rats [144], [169], Beagles [158] and minipigs [146].

However, some authors have reported unfavourable results after using simvastatin for bone formation. Lima *et al.* [170] found a negative impact of combining simvastatin with demineralized bovine bone matrix for repairing calvarial defects in rats after 30 to 60 days of healing. On postoperative day 60 the use of simvastatin, regardless of the dose, resulted in lower density than that observed in control and demineralized bovine bone matrix group samples.

Anbinder *et al*. also found that simvastatin administration, either orally or subcutaneously, did not improve bone repair for experimental tibial defects in rats [171].
Regarding the dosing of the simvastatin, caution should be exercised. Some authors have reported a dose-dependent inflammatory response [166]. In animal studies, a 0.1-0.5 mg dose of simvastatin would be the optimal dose for stimulating maximum bone regeneration without inducing inflammation [146].

Chapter 3
Materials and methods

Materials

All reagents used were of laboratory grade and purchased from Sigma-Aldrich, unless stated otherwise. Dextrin - Tackidex was from Roquette. Dextrin-VMA was synthesized by transesterification of dextrin with vinyl methacrylate (VMA), with few modifications from the protocol described by Ferreira *et al*. [172] for the transesterification of dextran with VA. In this work, dextrin-VMA with 20 acrylate groups per 100 dextrin glucopyranoside residues was used. Regenerated cellulose tubular membranes, were obtained from Membrane Filtration Products. All other chemicals and solvents used in this work were of the highest purity commercially available.

3.1 Glass reinforced hydroxyapatite (Bonelike) preparation

In the present study, Bonelike granules size ranging from 250 to 500 μm were prepared as follows. First, a P_2O_5-based glass with the composition of $65P_2O_5$-15CaO-$10CaF_2$-$10Na_2O$, in %mol, was prepared from reagent grade chemicals using platinum crucible at 1400ºC. The glass was ground and then the particles were sieved to a particle size less than 50 μm, using riddles with descending diameter. Medical grade hydroxyapatite was synthesized by chemical precipitation. After drying during 72 hours at 60ºC the hydroxyapatite was sieved until a particle size less than 75 μm was obtained. Then, the hydroxyapatite was mixed with the glass in a proportion of 2.5wt% [77], [81]. The mixed powders were dried for 24 hours at 60ºC and then sintered at 1300ºC for 1 hour. Finally, using, using standard crushing and sieving techniques the desirable particle range (250-500 μm) was obtained. The obtained hydroxyapatite was submitted to X-ray fluorescence spectrometry and X-ray diffraction (PANalytical, X'PERT-PRO model). Bonelike phase identification and quantification was performed using X-ray diffraction and Rietveld analysis.

3.2 Preparation of oDex Hydrogel

Dextrin Oxidation:

Briefly, aqueous solutions of dextrin (2% w/v) were oxidized with a 2 mL sodium m-periodate solution, to yield the theoretical degree of oxidation of 40%, at room temperature, with stirring, and in the dark. After 20 h, the oxidation reaction was stopped by adding dropwise an equimolar

amount of diethyleneglycol to reduce any unreacted periodate. The resulting solution was dialyzed for 3 days against water using a dialysis membrane with a molecular weight cutoff of 1000 Da and then lyophilized for 10 days. The degree of oxidation (DO) of oxidized dextrin (oDex) is defined as the number of oxidized residues per 100 glucose residues and was quantified using the tert-butylcarbazate method [105].

Preparation of oDex-ADH Hydrogels:

oDex was dissolved in PBS buffer (phosphate-buffered saline) (30% w/v) at room temperature, and an adipic acid dihydrazide (ADH) solution (prepared separately) was added at the concentration of 3,76% w/v. The cross-linking reaction was allowed to proceed during 30 minutes. The material was considered as gelified when it stopped slipping along a 90° inclined surface. The hydrogel preparation followed the protocol proposed by Molinos *et al*. [105].

3.3 Preparation of self-assembled nanoparticles of dextrin substituted with hexadecanethiol

For the nanoparticles preparation, the protocol proposed by Gonçalves *et al*. [131] was followed, as described ahead:

Synthesis of dexC16:

Dextrin-VMA and 1-hexadecanethiol were dissolved in dimethyl sulfoxide (equivalent VMA = 0.0413 M). A molar percentage of 1-hexadecanethiol (100% relative to VMA) were added to the reaction mixture in order to obtain the pretended degree of substitution (DS). Triethylamine (TEA) (1 mol equiv to VMA) was added to the reaction mixture. The medium was stirred for 24 h, at 50 ºC. The mixture was dialysed for 48 h against water with frequent water change. After freezing, the mixture was lyophilized and stored.

Sample preparation:

Lyophilized dexC16 was dissolved in water or PBS under stirring at 50 ºC until a clear solution was obtained. The degree of solubility of dexC16 depends on the degree of substitution. Increasing the degree of substitution reduces the solubility. In the range of DSC16 used, to prepare a 1.0 g/dL solution, 3 h of stirring is the maximum time required to dissolve dexC16.

Dynamic light scattering:

The size distribution was determined with a Malvern Zetasizer, Model Nano ZS (Malvern Instruments Limited, U.K.). A dispersion of nanoparticles in water (1 mL) was analysed at 25 ºC in a polystyrene cell using a Helium-Neon laser – wavelength of 633 nm and a detector angle of 173º. The dispersion was filtered through a 0.22 µm pore.

^{1}H NMR:

Lyophilized dexC16 was dispersed in deuterium oxide (1.0 g/dL). Solutions were transferred to 5 mm NMR tubes. 1D ^{1}H NMR measurements were performed with a Varian Unity Plus 300 spectrometer operating at 299.94 MHz. 1D ^{1}H NMR spectra were measured at 298 K with 80 scans, a spectral width of 4800 Hz, a relaxation delay of 1 s between scans, and an acquisition time of 3.75 s.

3.4 Preparation of the oDex-Nanogel Hydrogels and Bonelike-oDex-Nanogel Hydrogels

oDex, DO 40%, (30% w/v) was dissolved in PBS or in a suspension of nanogel for ~16 h at room temperature. Then, the oDex suspensions were mixed with 5% (in molar base taking into account the number of glucose residues in the original dextrin) ADH. The cross-linking was allowed to proceed at room temperature for 30 minutes. Ahead, the oxidized dextrin hydrogels are termed as oDex hydrogels, and the oxidized dextrin hydrogels with incorporated dextrin nanogels are called oDex-nanogel hydrogels.
For the Bonelike-oDex-Nanogel Hydrogel, the same protocol was followed, but before adding the ADH, Bonelike (60% or 40% w/v) was added to the samples and stirred. Then, ADH was added to each sample and the cross-linking was allowed to proceed at room temperature for 30 minutes.

3.5 Cryo-Scanning Electron Microscopy (Cryo-SEM) Analysis

The topography and porosity of the injectable bone graft substitutes (30% w/v oDex, 10 mg/mL nanogel and 40 or 60% w/v Bonelike) were studied by Cryo-SEM.
The SEM / EDS analysis was performed using a High Resolution Scanning Electron Microscope with X-Ray Microanalysis and CryoSEM experimental facilities: JEOL JSM 6301F/ Oxford INCA Energy 350/ Gatan Alto 2500. The samples (n=3) were rapidly cooled (plunging it into sub-cooled nitrogen – slush nitrogen) and transferred under vacuum to the cold stage of the preparation chamber. The specimens were fractured, sublimated ('etched') for 90 seconds at -90°C, and coated with Au/Pd by sputtering for 45 seconds and then transferred into the SEM chamber where were studied at a temperature of -150°C.

3.6 Injectability tests

The injectability tests were conducted at the Faculty of Pharmacy, University of Porto. The equipment TA.XT2*i* Texture Analyser was used to evaluate the extrusion force of injectables, in order to determine if they can be applied in a clinical environment. The tests were performed in triplicate per each testing condition. 1mL samples of the Injectable Bonelike-oDex-Nanogel Hydrogel were placed inside 2mL syringes, followed by a 30 minutes period to allow the cross-linking reaction. The syringes were fixed vertically to the bottom plate and the equipment applied the necessary force to move the plunger 1 mm/s in the syringe. The results were expressed as the force required to move the plunger out of the syringe.

3.7 Preparation of simvastatin-loaded Bonelike scaffolds and *in vitro* assay of simvastatin release

Simvastatin was dissolved in pure ethanol at a concentration of 5mg/mL. For the preparation of simvastatin-loaded Bonelike scaffolds, 100µl of the previous solution was dropped onto Bonelike under sterile conditions, and then allowed to dry completely in a laminar flow hood for 24 h. 2 groups of samples were prepared (n=3), containing 60 mg of Bonelike and 0 mg or 0.5mg simvastatin, respectively.
The scaffolds (60 mg) were placed in 1 ml PBS at 37°C at 60 rpm. At 24, 48, 72, 96, 168, 192, 216 and 240 hours, the PBS was changed. At every time-point the solution absorbance was measured at a wavelength of 238 nm using an ultraviolet-visible spectrophotometer, while the

simvastatin concentration was determined from a standard curve prepared with various amounts of simvastatin.

3.8 Incorporation of simvastatin in the nanogel

Simvastatin (SIM) was loaded into the hydrophobic domains of nanoparticles. The physical entrapment of simvastatin in the nanoparticles was performed following the nanoparticles formation, as described ahead. 2 stock solutions of simvastatin in ethanol with a concentration of 5 mg/mL and 10 mg/mL were prepared. The required volume of simvastatin from these solutions was added to the nanoparticles solutions (final concentration of ethanol < 1%). The effect of polymer/simvastatin ratio on the loading efficiency and stability of the formulation was studied. Different formulations were prepared by varying the concentrations of simvastatin (5 mg/mL and 10 mg/mL) and polymer (1.0 and 3.0 mg/mL). In order to evaluate the entrapment efficiency, the solutions were kept under stirring during predeterminated times (3 and 24 hours). The resultant solutions were centrifuged at 10000 rpm, for 5 min, to remove the insoluble simvastatin. The supernatants were carefully collected and analyzed spectrophotometrically. The quantification was carried out using a calibration plot obtained with different simvastatin concentrations. The entrapment efficiency was calculated by the Equation 3.1:

$$Entrapment\ efficiency\ (\%) = \frac{[Simvastatin]\ encapsulated}{[Simvastatin]\ added} \times 100\ , \quad \text{(equation 3.1)}$$

The size distribution of unloaded and loaded dextrin nanoparticles was determined by dynamic light scattering (DLS) using a Malvern Zetasizer, Model Nano ZS. The nanoparticles dispersion was analysed at 25ºC in a polystyrene cell, using a He-Ne laser - wavelength of 633 nm and a detector angle of 173º. The DLS analysis provides the characterization of a sample through the mean value (z-avg) for the diameter, and a width parameter known as the polydispersity index (PdI).

3.9 *In vitro* assay of simvastatin release from the nanogel

The release of simvastatin from the nanoparticles was studied using sink conditions. The simvastatin loaded nanoparticles (5mg/mL of simvastatin and 1.0 mg/mL of polymer in an aqueous solution) was placed in a dialysis membrane.

The dialysis membrane (molecular cut off of 2 kDa) was placed in 200 mL of PBS, shaken under 250 rpm at 37ºC. At predefined timeframe (up to 24 h), a sample of 200 µL was withdrawn, centrifuged to guarantee removal of unentrapped simvastatin and the supernatant was analyzed spectrophotometrically.

3.10 Materials sterilization

Sterilization of Bonelike granules was performed by autoclaving the material during 35 minutes, at 121ºC. oDex hydrogel was sterilized by UV light, during 1 or 2 hours. To acess the efficacy of this method, sterilized samples (n=3) were immersed in αMEM during 4 weeks. The dextrin nanoparticles were sterilized by filtrating the dispersion through a 0.22µm pore (Sterile Cellulose Acetate Membrane, Frilabo).

3.11 MTT assay

Mouse embryo fibroblasts 3T3 (ATCC CCL-164) were grown in Dulbecco's modified Eagle's media supplemented with 10% newborn calf serum (Invitrogen, U.K.) and 1 µg/mL penicillin/streptavidin (cDMEM) at 37 °C in a 95% humidified air containing 5% CO2. Before reach confluency, 3T3 fibroblasts were harvested with 0.05% (w/v) trypsin-EDTA and subcultivated in the same medium.

The cytotoxicity of the nanoparticles unloaded and loaded with simvastatin was assessed in a 3T3 fibroblasts culture previously incubated for 24 h (2.0 × 104 cells/well, in a 24-well polystyrene plate, n=3) using 3-[4,5-dimethylthiazol-2-yl]-2,5-diphenyl tetrazolium bromide (MTT) assay, as described ahed. The nanoparticles were sterilized and dissolved in cDMEM. Increasing concentrations of loaded and unloaded nanoparticles (0.5, 0.75, 1 and 2 mg/mL) dissolved in cDMEM at 20% (v/v), were then added to the fibroblast culture. Free simvastatin, in the same concentration that was incorporated in the nanoparticles, was dissolved in cDMEM at 1% (v/v). After 24h and 48 h of incubation, cell viability was accessed by MTT assay. Morphological evaluation of 3T3 cells was also made by regular light microscope observations.

3.12 *In vivo* tests

The objective was to observe ectopic bone formation in subcutaneous implants in rats, due to simvastatin action, during an 8-week experiment. The injectable composite materials were sterilized by the methods previously referred.

100 µl of samples were surgically implanted subcutaneously in the lumbar region of three male rats (Sasco Sprague Dawley, Barcelona, Spain, weighting around 300 g), each one receiving 5 implants with the following scheme:

Figure 3.1 - Implant scheme: (1) oDex-nanogel/SIMV hydrogel; (2) oDex-nanogel/SIMV hydrogel + MSCs; (3) oDex-nanogel hydrogel; (4) oDex-nanogel hydrogel + MSCs; (5) Bonelike/SIMV-oDex hydrogel;

Previous experimental work already evaluated the biological response of rats using a control with no implant where the suture was performed (Sham group). Two animals were housed per cage (Makrolon type 4, Tecniplast, VA, Italy), in a temperature and humidity controlled room with 12-12h light/dark cycles, and were allowed normal cage activities under standard laboratory conditions. The animals were fed with standard chow and water ad libitum. Adequate

measures were taken to minimize pain and discomfort taking into account human endpoints for animal suffering and distress.

All procedures were performed with the approval of the Veterinarian Authorities of Portugal, and in accordance with the European Communities Council Directive of November 24th 1986 (86/609/EEC). Anaesthesia was achieved with an intraperitoneal injection of a pre-mixed solution consisting in ketamine (Imalgene 1000R), 100 mg/kg body weight, and xylazyne (RompunR), 200 mg/kg body weight. Hair from the dorsal area was clipped and the skin scrubbed in a routine fashion with an iodopovodone 10% solution (BetadineR). Five 1.5-2cm long linear incisions were performed. After blunt dissection towards the ventral aspect of the body, the biomaterials were implanted subcutaneously. Skin and subcutaneous tissues were closed with a simple-interrupted suture of a non-absorbable filament (SynthofilR, Ethicon).

Chapter 4
Results and Discussion

4.1 Glass reinforced hydroxyapatite (Bonelike) preparation

The obtained hydroxyapatite was submitted to X-ray fluorescence spectrometry to perform a chemical and elemental analysis. X-ray diffraction was used to identify and quantify the different crystalline phases. The values of the tables 4.1 and 4.2 are inside the range of values of the norm ISO/DIS 13779-1 (Implants for surgery — Hydroxyapatite; Part 3: Chemical analysis and characterization of crystallinity and phase purity) [173].

Table 4.1 - Quantitative chemical analysis of the hydroxyapatite[1].

Analytical parameter	Obtained value	Uncertainty	Units
Arsenic (As)	<1.0 q.l. *1	n.a. *2	mg/Kg
Cadmium (Cd)	<0.5 q.l. *1	n.a. *2	mg/Kg
Mercury (Hg)	<0.5 q.l. *1	n.a. *2	mg/Kg
Lead (Pb)	<0.5 q.l. *1	n.a. *2	mg/Kg
Ca/P	1.68	n.a. *2	Molar ratio

Table 4.2 - Quantification of crystalline phases by X-ray diffraction of the hydroxyapatite.

Crystalline phases	Chemical formula	wt%	Uncertainty
hydroxyapatite	$Ca_{10}(PO_4)_6(OH)_2$	99	±2
α tricalcium phosphate	$Ca_3(PO_4)_2$	<1 q.l. *1	n.a. *2
β tricalcium phosphate	$Ca_3(PO_4)_2$	<2 q.l *1	n.a. *2
calcium oxide	CaO	<1 q.l. *1	n.a. *2
tetracalcium phosphate	$Ca_4(PO_4)_2O$	<2 q.l. *1	n.a. *2

*1 q.l. quantification limit; *2 not applicable;

As table 4.1 shows, the molar ratio was the expected for hydroxyapatite and very similar to the human bone Ca/P molar ratio (1.631) [174].
During the sintering process of Bonelike, the CaO-P_2O_5 glass (also produced for this work) reacts with hydroxyapatite, forming β-tricalcium phosphate, which then can transform into α-tricalcium phosphate at higher temperatures. Figure 4.1 display an X-ray diffraction pattern of Bonelike [81]. Rietveld analysis previously reported indicated that Bonelike is composed by 68.4% of hydroxyapatite, 24% of α-TCP, and 7.6% of β-TCP [81], [175], [176].

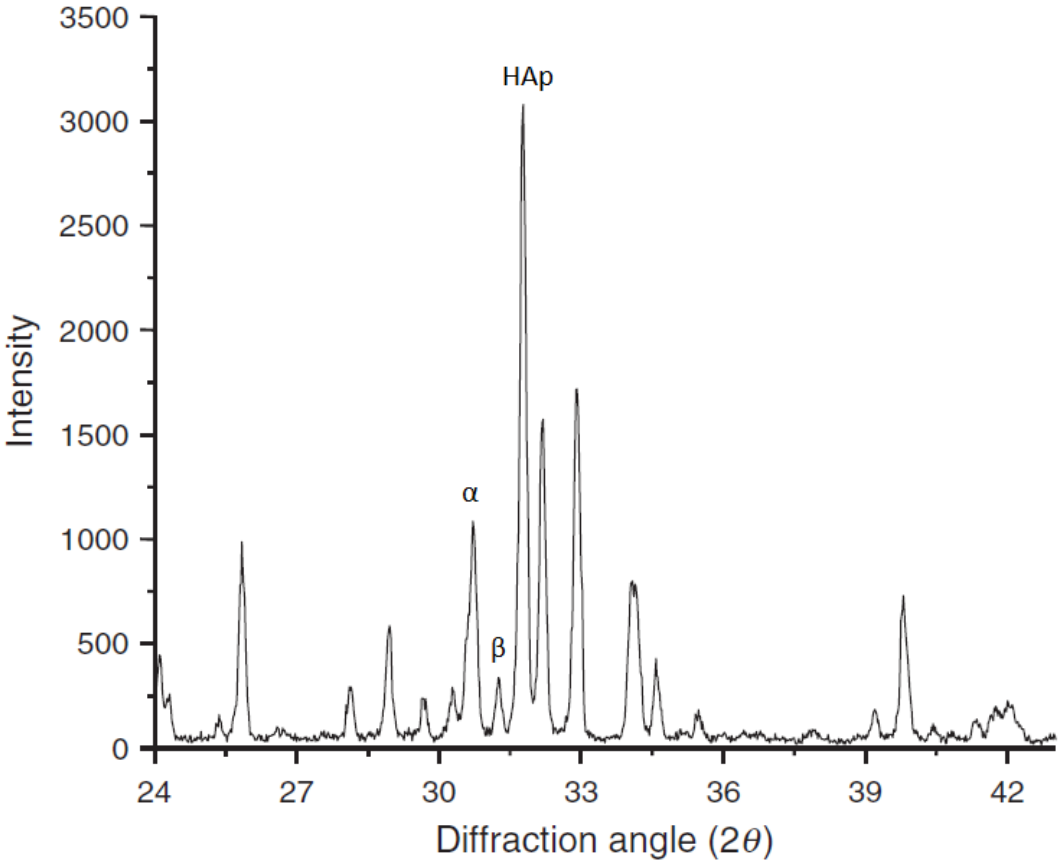

Figure 4.1 - X-ray diffraction pattern of Bonelike, which is composed of hydroxyapatite (HAp), α-TCP (α) and β-TCP (β) [81].

Bonelike has been reported to be osteoconductive and bioactive, supporting the formation of mechanically and chemically bonded bone directly on its surface [49], [51], [177]-[179]. A balance between the least soluble phase of hydroxyapatite and most soluble phase of tricalcium phosphate determines the bioactivity of Bonelike. Due to the presence of biodegradable α and β-TCP phases in the structure of Bonelike, a local enrichment in Ca and P in the physiological environment occurs, which stimulates new bone formation [175]. For this work, Bonelike with granules size ranging from 250 to 500 mm, as shown in figure 4.2, was obtained using using standard crushing and sieving techniques. A porosimetry of 65% for the Bonelike produced was reported previously, in our lab, using mercury intrusion porosimetry analysis.

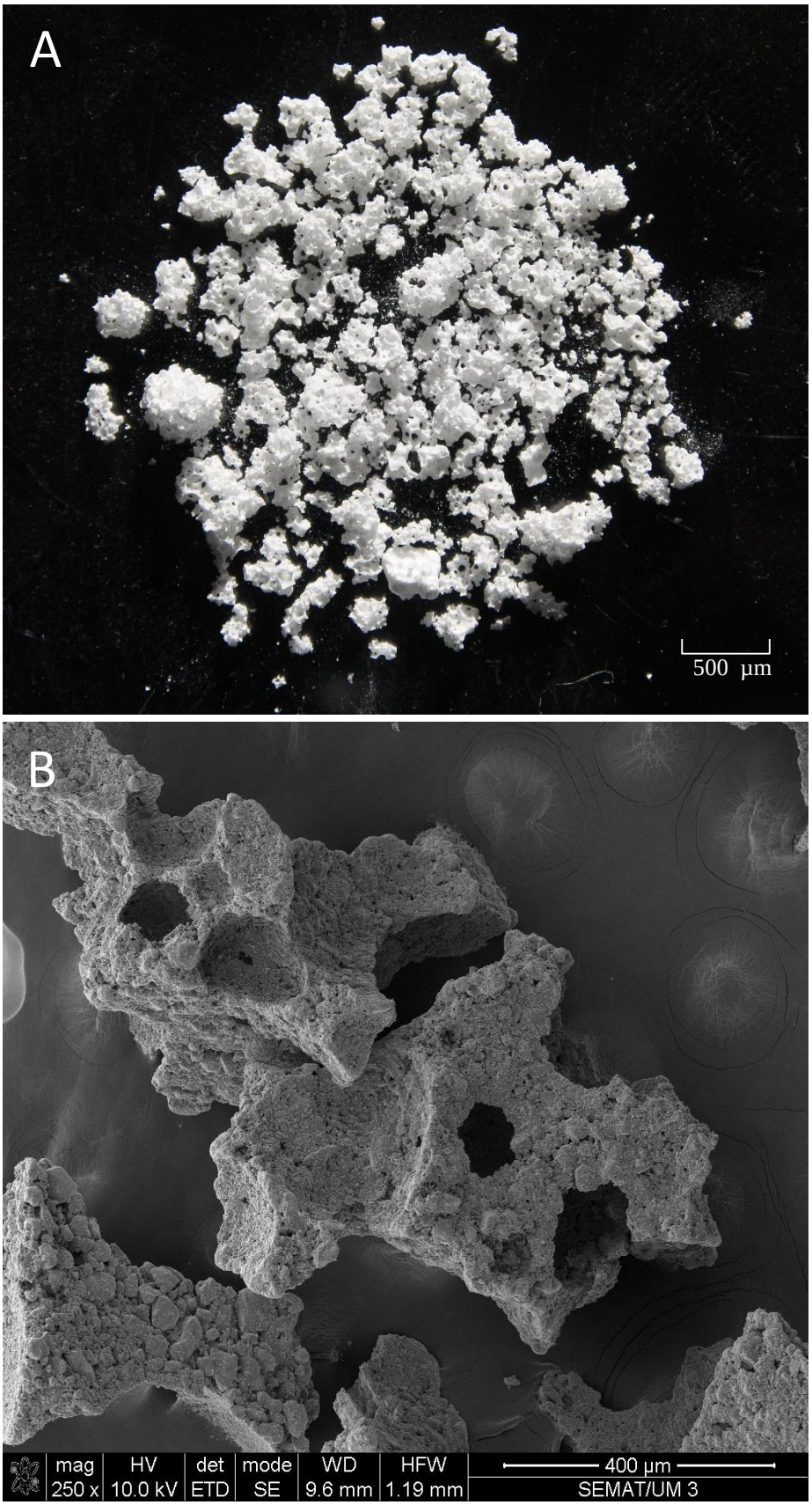

Figure 4.2 - Glass reinforced hydroxyapatite (Bonelike) with a particle size from 250 to 500 µM; (A) macroscopic aspect of Bonelike granules and (B) SEM image showing the surface morphology.

The preparation of the Bonelike scaffold followed the standard protocol reported previously [77], [175].

4.2 Preparation of oDex Hydrogel

Since the oDex hydrogel was already well studied and published [105], [107], [125], [130], the conditions that best fulfill the requirements for the final application of this work were chosen from the literature. Since the ultimate goal is the *in vivo* implantation, the cytotoxicity of the hydrogels was taken into account. The cytotoxicity of the oDex hydrogels, was evaluated and reported for the reticulating agent (ADH), oDex hydrogels, as well as its degradation products and the overall results point to the oDex hydrogels cytocompatibility [105].

Through control of DO and ADH concentration, a good control over the gelation time was possible. A gelation time too long would make the injectable system inappropriate to use in clinical aplications, as it would unnecessarily prolong the time of medical protocols and consequently increase the cost of treatment. This would be impractical in clinical environment. However, if the gelation time is too fast, it will prevent a good homogenization of the material, making difficult to obtain materials with reproducible characteristics. DO of 50% would originate gelation periods inferiors to 1 minute and DO of 32,5% gelation periods of 30 minutes. In the range of values already tested [105], 40% was the chosen one, having gelation periods of around 2 minutes.

4.3 Preparation of self-assembled nanoparticles of dextrin substituted with hexadecanethiol

According to the protocol proposed by Gonçalves *et al*. [134], ^{1}H NMR was used to analyse the structure of the reaction product. The signals between 5.8 and 3.0 ppm in the ^{1}H NMR spectrum of dextrin are assigned to protons from the dextrin scaffold (Figure 4.3). As shown in this figure, the protons from the acrylate group, attached to the dextrin backbone are observed between 1.9 and 2.1 ppm and 6.6 and 6.0 ppm [172].

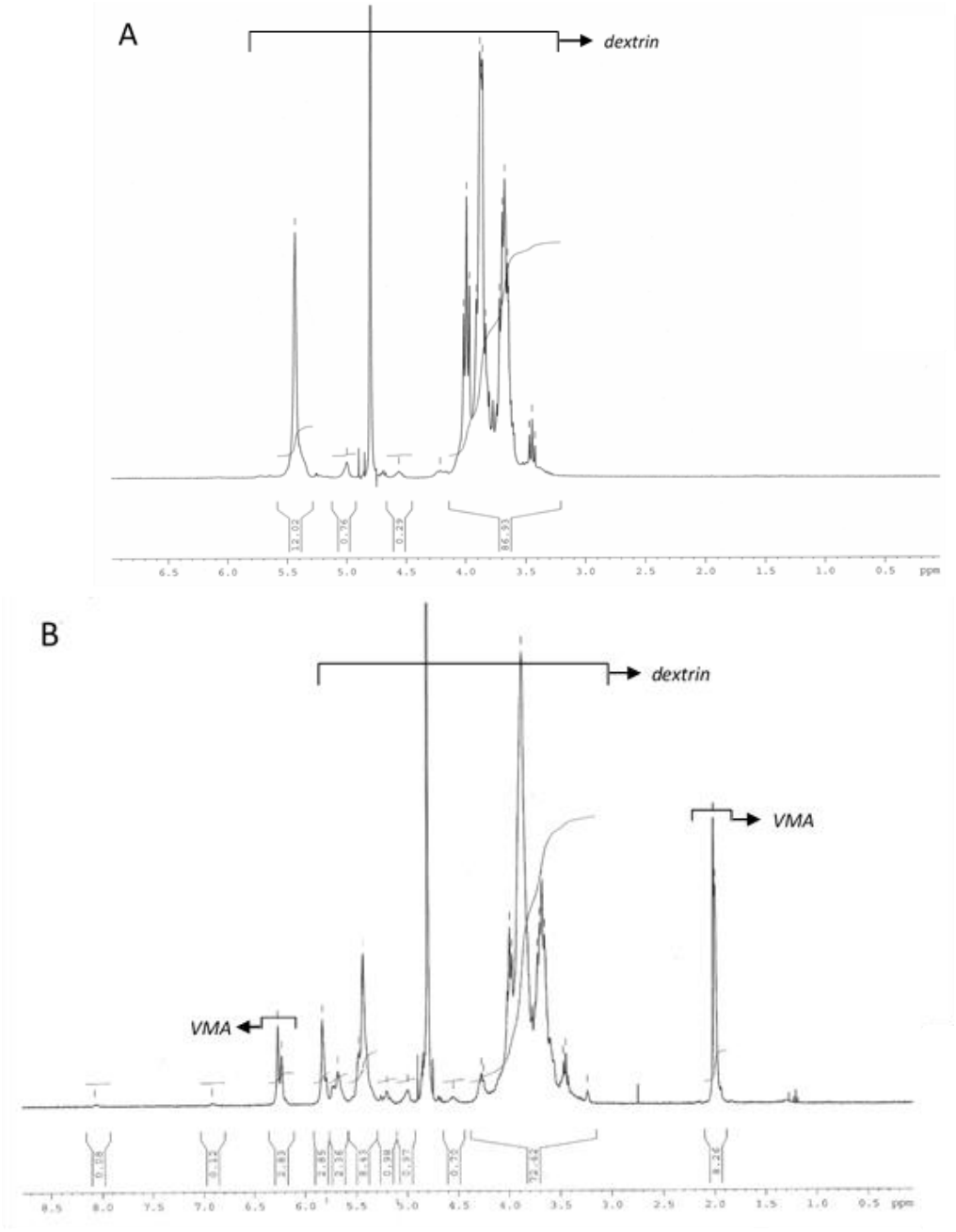

Figure 4.3 - ^{1}H NMR spectra of (**A**) dextrin and (**B**) dextrin-VMA (DS_{VMA} 24%) in D_2O at 25ºC.

The reaction between the grafted acrylate and the thiol hexadecanethiol follows a mechanism of Michael addition [134] . The intensity of the signals from protons of the unsaturated carbons of the acrylate groups decreases as the reaction progresses, and the signals should eventually disappear completely when all acrylate groups are grafted with thiol moieties. Simultaneously, a new signal assigned to the methylene protons should appear.

Although it was possible to identify the signals corresponding to the grafted alkyl moiety, between 2.0 and 0.6 ppm, the acrylate protons are still detected. Using TEA as a catalyst, the signals from thiol moieties have higher intensity and the acrylate signals completely disappear, confirming the success of the synthesis (Figure 4.4).

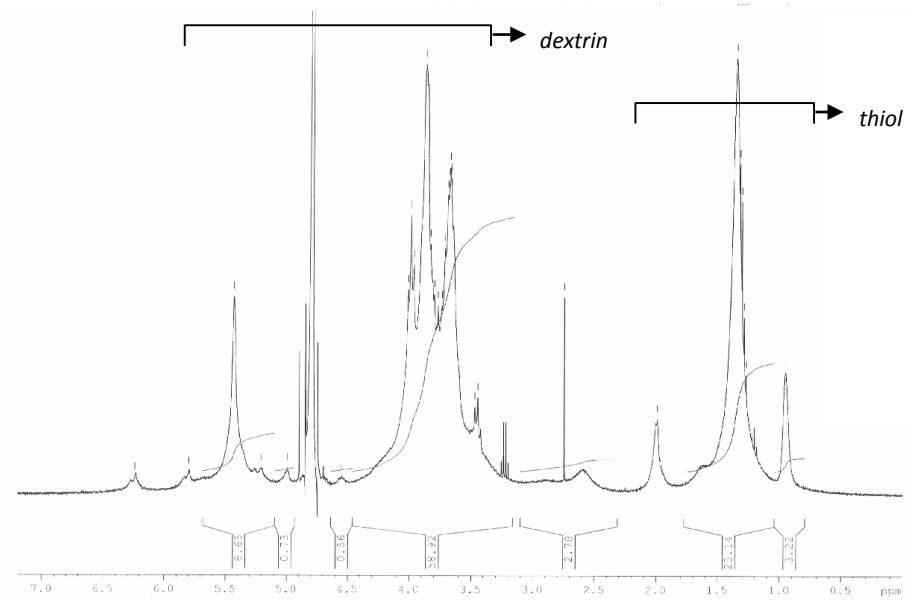

Figure 4.4 - ^{1}H NMR spectra in D_2O of dextrin-VMA reacted with hexadecanethiol with TEA.

The ^{1}H NMR spectrum of dexC16, in deuterated water, was used to determine the degree of substitution obtained (DSC16, amount of alkyl chains per 100 dextrin glucopyranoside residues). DSC16 was calculated as a peak area ratio in the NMR spectra, according to Equation 4.1:

$$DS\ C16 = \frac{7 \times x}{37 \times y} \times 100\,, \qquad \text{(Equation 4.1)}$$

where x is the average integral corresponding to the protons from alkyl moieties (2.0 - 0.6 ppm) and y is the integral of all dextrin protons (3.0 - 5.8 ppm). In this work, the DS_{VMA} was 24% and DS_{C16} was 7%. Despite the nanoparticle size is only shlighty influenced by DS_{C16} [135], it has been already reported that with DS_{C16} 7%, the mean diameter of nanoparticles ir roughly 20nm (determined by DLS and AFM) [134]. The nanoparticles also remain stable up to two months, wich means that the particles kept their size and indicate the high colloidal stability of nanoparticles in the aqueous medium [135]. Small size, low density and high stability of the nanoparticles produced can promote a stable entrapment of bioactive and hydrophobic molecules, like simvastatin [135], [139].

4.4 Preparation of the oDex-Nanogel Hydrogels and Bonelike-oDex-Nanogel Hydrogels

The development of the injectable hybrid hydrogels consists in mixing glass reinforced hydroxyapatite (Bonelike) and oDex hydrogel to obtain a compact compound. Different combinations such as dextrin nanogel + oDex hydrogel and Bonelike + dextrin nanogel + oDex hydrogel were prepared for some tests. Two different ratios (40 and 60%) of hydrogel / Bonelike were studied. During the preparation of the samples for the Cryo-SEM analysis, a high concentration of dextrin nanoparticles was used to improve the chances of being observed during the analysis. It was observed macroscopically that the formulations with only oDex-nanogel hydrogel, with a nanogel concentration of 10mg/mL, result in improved mechanical properties (figure 4.5). The material showed improved capacity to maintain a predetermined form and a greater cohesion

when compared with Bonelike-oDex hydrogel (figure 4.6). According to the literature [105], [180]–[182], this can be attributed to a further reticulation of the hydrogel network.

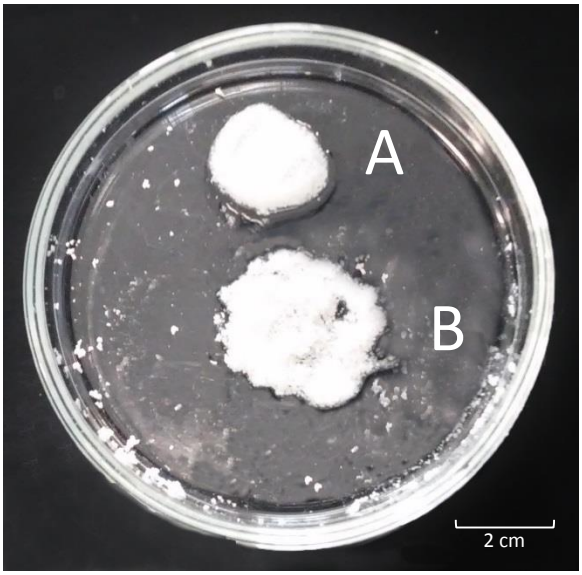

Figure 4.5 - Macroscopic aspect of (**A**) Bonelike oDex-nanogel hydrogel, with 10mg/mL of dextrin nanoparticles and (**B**) Bonelike oDex hydrogel.

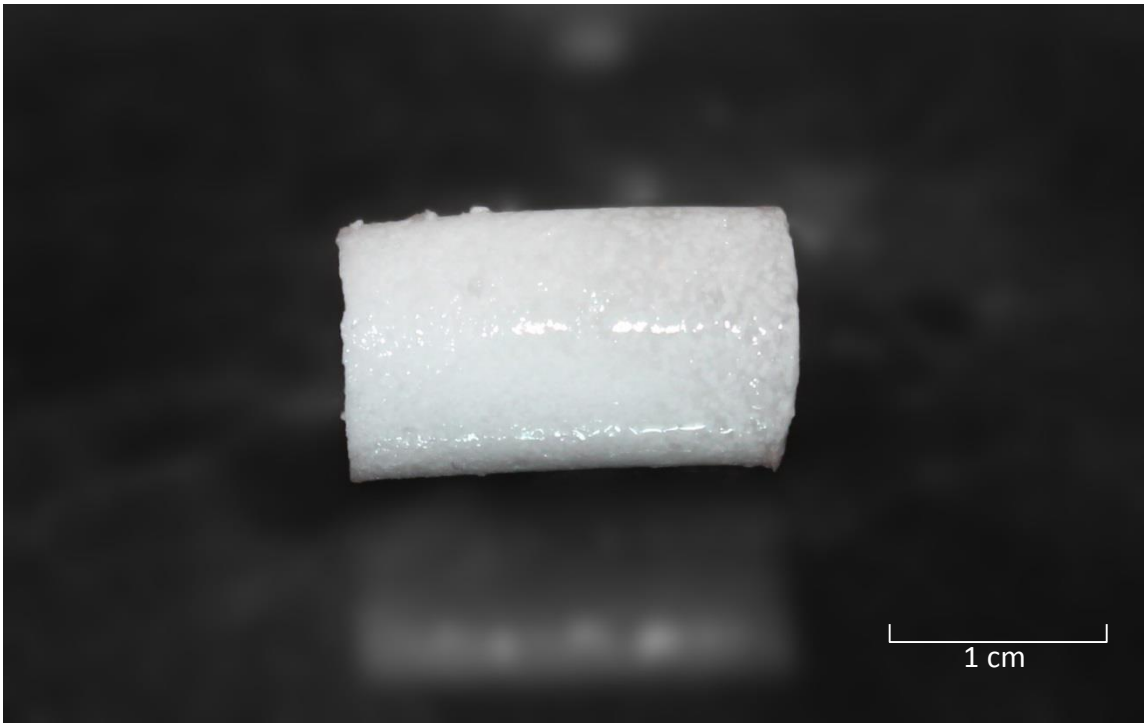

Figure 4.6 - Bonelike oDex-nanogel hydrogel.

For the injectability tests the same concentration of nanogel (10mg/mL) was used to determined if the extrusion force would be significally different. Although mass loss studies protocols

for this kind of materials show low fiability when the results are transposed to in vivo implantation, it is already known that the degradation speed of oDex hydrogels is different from the oDex-nanogel hydrogels. It is expected that the oDex-nanogel hydrogel have a degradation 30% slower than the one observed in oDex hydrogels [105]. According to mass loss studies already published for oDex hydrogel, in approximately 25 days, the oDex hydrogel network is completely solubilized, whereas only ~70% mass loss was observed in oDex-nanogel hydrogels (nanogel concentration of 3mg/mL). However, these results correspond to a study where dextrin *Koldex 60 starch* was used. For this work, a medical grade dextrin was used, *Tackidex*. Very recently, it was reported that the degradation time for oDex hydrogels made with dextrin *Tackidex* was of 24 hours, *in vitro* [183]. The *in vitro* protocols involve mechanical manipulation of the hydrogels, inducing a faster degradation than the ones that occur *in vivo*.

The relatively quick degradation rate of the Tackidex hydrogel is suitable for the purpose of this work where the hydrogel have to perform as an injectable carrier of Bonelike granules.

Regarding the gelation time, it was noted that after adding the reticulating agent to the formulation with Bonelike, nanogel and hydrogel (injectable Bonelike-oDex-nanogel hydrogel), the approximate gelation time for the DO of the hydrogel (40%) was a little higher than the one reported in the literature [105], [125]. It was reported gelation times of around 2 minutes, while during the preparation, with the conditions tested, gelation times between 8 and 15 minutes were observed. This difference is due to the ceramic granules of Bonelike, which slow the gelation time. In fact, the optimal gelation time range suggested by surgeons has been defined between 5 and 30 minutes [184]. Therefore, for the purpose of this work, this increase in the gelation time will allow that at the time of implantation, the surgeon can choose between a more viscous or more fluid material, that reticulate inside the syringe or *in situ*, respectively. This represents very promising and suitable characteristics for the application of the injectable in clinical environment.

4.5 Cryo-Scanning Electron Microscopy (Cryo-SEM) Analysis

The dextrin nanogel and the Bonelike granules were incorporated in the oDex hydrogel, and the hybrid hydrogel was further characterized. Cryo-SEM analysis was used to examine the morphologies of the injectables. As shown in figure 4.7 and described in literature [105], the covalent cross-linking of the hydrogel produced tridimensional networks with a porous structure, with a diameter of ~1µm.

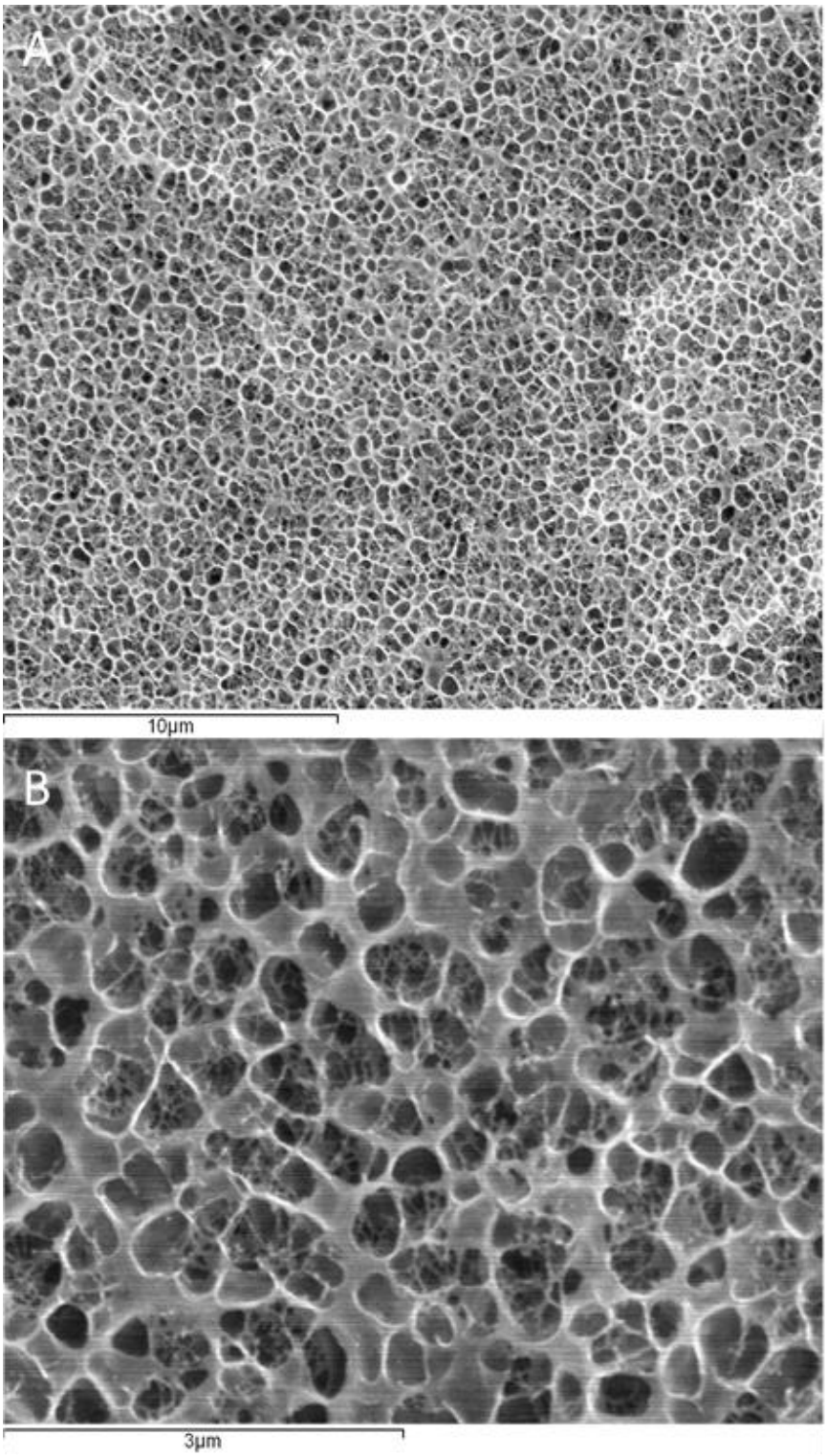

Figure 4.7 - (A) Cross-section of oDex hydrogel and (**B**) detail of the porous structure.

The Bonelike granules were completely and successfully incorporated in the hydrogel and remained easily suspended in the hydrogel matrix (figure 4.8). Using larger amplifications, the nanogel particles can be observed in the matrix of the hydrogel (figure 4.9).

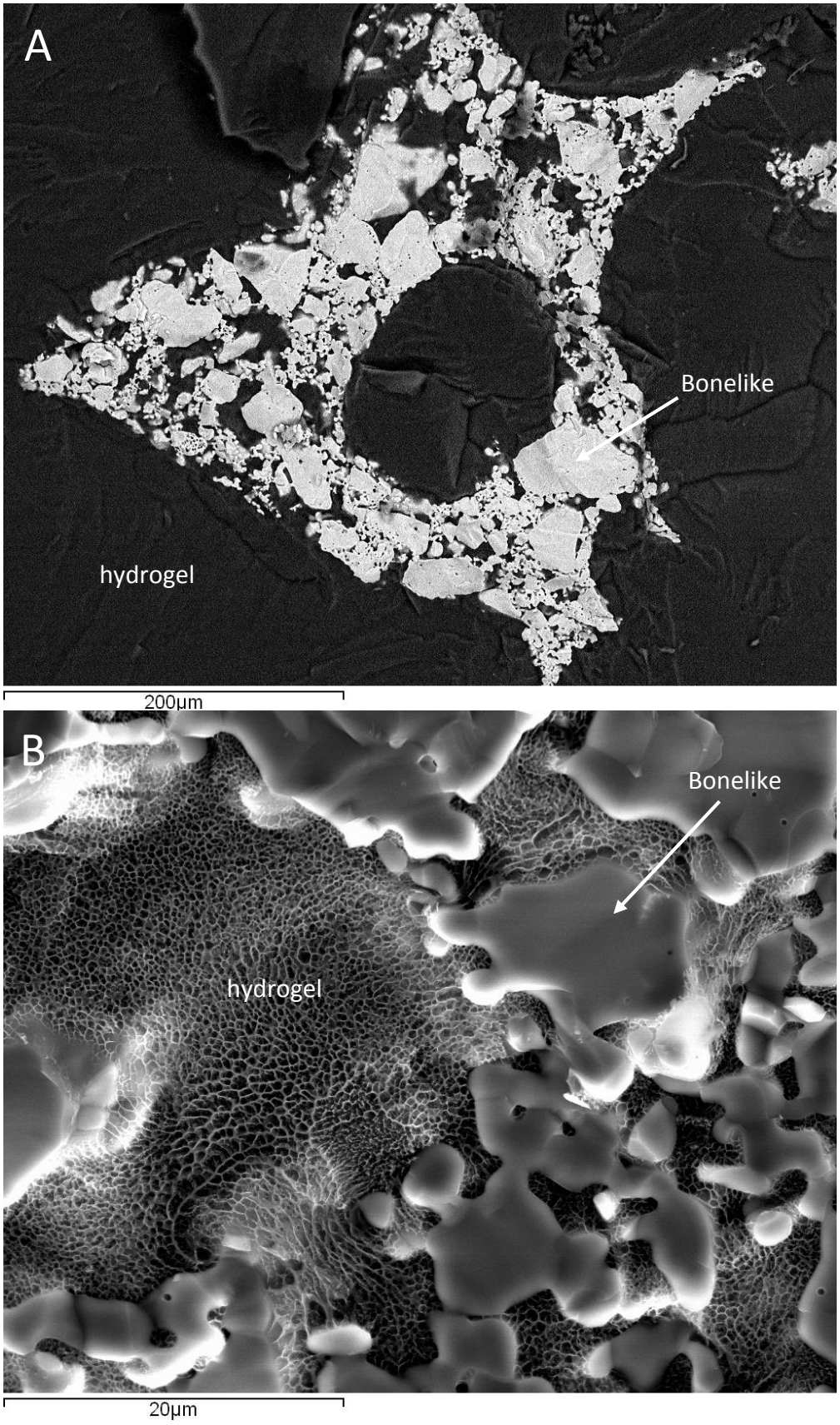

Figure 4.8- Cryo-SEM images from cross-section of **(A)** Bonelike granules completely embedded in the hydrogel matrix and (**B**) detail of the porous structure of the hydrogel inside Bonelike.

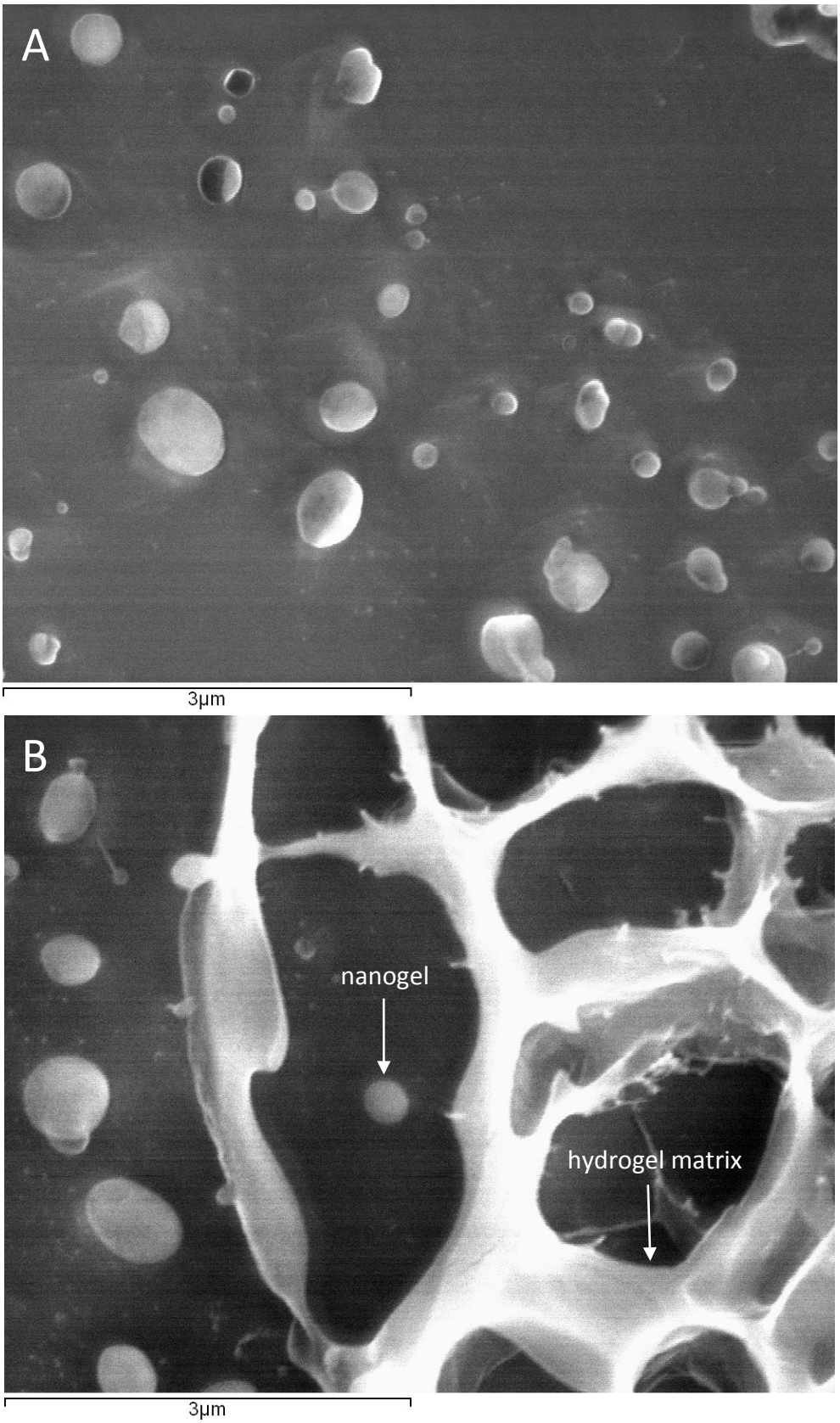

Figure 4.9 - Cryo-SEM images from (**A**) dextrin nanoparticles and (**B**) dextrin nanoparticles inside the oDex hydrogel matrix.

No morphological differences were noted comparing the oDex and oDex-nanogel hydrogel formulations. As expected, the incorporation of the nanogels and the Bonelike granules did not have significant influence in the morphology of the oDex hydrogel network.
The material produced is a three-dimensional, highly porous structure with interconnected porosity, displaying characteristic that will serve as scaffold for tissue growth.

4.6 Injectability tests

During the injection of a formulation via a needle, the force applied to a syringe plunger is dissipated in three ways: (1) overcoming the resistance force of the syringe plunger; (2) imparting kinetic energy to the formulation; and (3) forcing the formulation through the needle [185]. The third topic should be adapted to the protocol that was performed in this work. The formulation was not extruded through a needle due to one main reason: having a formulation with ceramic granules does not allow the extrusion through the typical syringe with a needle of very small diameter, due to the size of the granules.
In the tests performed, the top of the syringe was cutted, according preliminary tests. This was done not only due to the already referred reasons but also to allow comparing the results with other tests performed by our group, using different materials (data not shown). In figure 4.10, the results obtained for four diferent conditions are shown. As expected, the conditions with the Bonelike granules showed a higher extrusion force than using formulations just composed by oDex-nanogel.

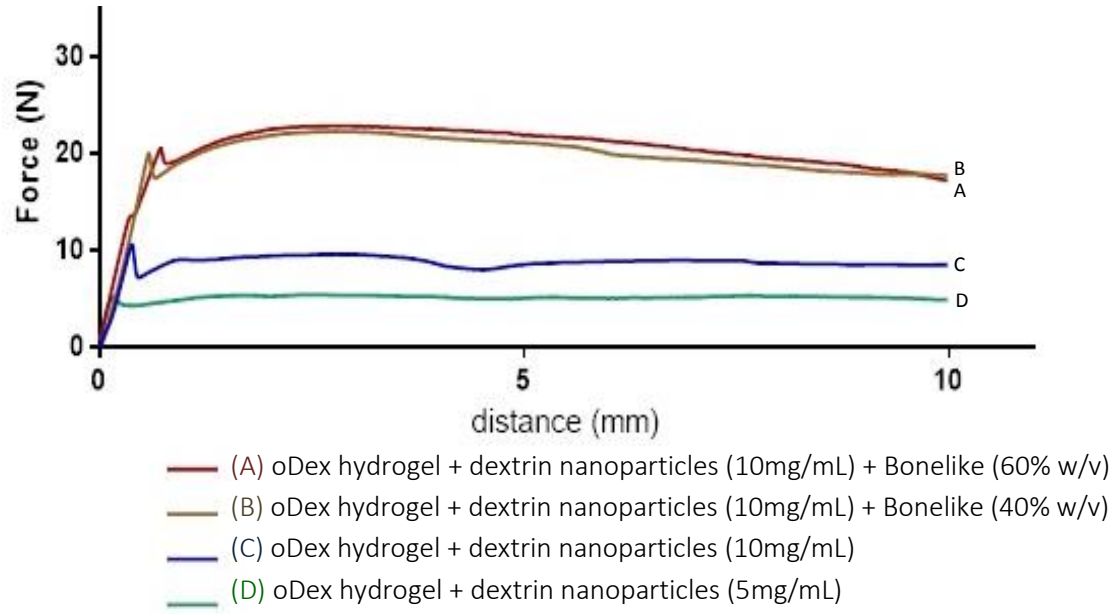

Figure 4.10 - Extrusion profiles for the different injectables.

Table 4.3 - Injectability tests results.

Injectable	Maximum extrusion force [N]	Average force of plateau area [N]
A	29,15	20,93 (±5,15)
B	26,39	20,15 (±7,36)
C	10,64	8,87 (±0.40)
D	5,46	5,22 (±0.73)

In table 4.3 is shown the maximum extrusion force and the average of plateau area (±SD), obtained for the course between 2 and 10 mm. Statistical analysis using One Way Repeated Measures ANOVA, indicated that no statistical diference existed between A and B and between C and D. For the other combinations (A/C, B/C, A/D and B/D), existed significant statistical differences ($p<0.05$). The standard deviations for the conditions that contained Bonelike are relatively high when compared with the conditions where there was no Bonelike. This is due to different degrees of compaction of the material inside the syringe and small air bubbles that entered during the homogenization. The main purpose of this trial was to study the extrusion forces when using the maximum concentration possible of dextrin nanoparticles (10mg/mL) in the Bonelike and oDex hydrogel. Due to the nature of the assay, which requires large amounts of material, only the four conditions were analysed; in this way, we would get the maximum value of extrusion for the future formulations with nanoparticles.
When these results are compared with other test performed in our lab, some conclusions arise. Preliminary assays, showed that oDex hydrogel have an average extrusion force of 3,91 N ((±0.66). Adding dextrin nanoparticles to the formulation, increased the extrusion force for 5,22 N (±0.73) and 8,87 N (±0.40), at 5mg/mL and 10mg/mL, respectively. This was already expected due to macroscopic observation. According literature, this is assigned to a further reticulation of the hydrogel network [105], [180]–[182].
As expected, the conditions incorporating Bonelike in the hydrogels presented higher extrusion forces, due to the ceramic granules. Preliminary data, showed that the combination of oDex hydrogel + Bonelike (60% w/v) and oDex hydrogel + Bonelike (40% w/v) have an average force, in the plateau area, of 6,09 N (±0.51) and 4.74 N (±0.34), respectively. This demonstrates that the nanogel, at very high concentrations, significantly increases the composite extrusion forces. Khairoun *et al*. [186], [187] measured the injectability of a calcium phosphate bone cements and the force required to extrude reach values larger than 100 N, and hence was declared non-injectable [188]. In this work, the results suggest that the formulations easily allow a surgeon to perform a smoothly extrusion of the material through a syringe thereby ensuring the injectability of the hybrid material produced.

4.7 Preparation of simvastatin-loaded Bonelike scaffolds and *in vitro* assay of simvastatin release

Very recent studies have successfully incorporated simvastatin in hydroxyapatite fiber [147] and calcium sulphate scaffolds [159], and reported that combinations of this scaffolds and

simvastatin stimulated new bone formation in a dose-dependent manner. Previous studies have investigated the effects of the local application of simvastatin. Stein et al. [189] reported that 0.5 mg simvastatin appeared to be the optimal dose for single local application and this dose produced the best bone growth/inflammation ratio. In a study by Wong et al. [190], an aqueous solution with 0.5 mg of simvastatin was added to a collagen matrix in calvarial defects in rabbits and a 308% increase in new bone was present in the simvastatin-collagen group compared with the collagen group alone at the end of 14 days. Based on these findings, this line of investigation was followed: simvastatin was used as growth-factor-like substance and Bonelike as scaffold. Based in previous reports [147], [159], [189], [190], 0.5 mg simvastatin was selected and incorporated into the Bonelike scaffolds for the in vitro release assays.
The *in vitro* release pattern of simvastatin from the simvastatin-loaded Bonelike is shown in figure 4.15. In the first 24 hours, ~5.5% of simvastatin was release from the scaffold; this percentage of drug correspond to the solubility limit of simvastatin in the medium used.

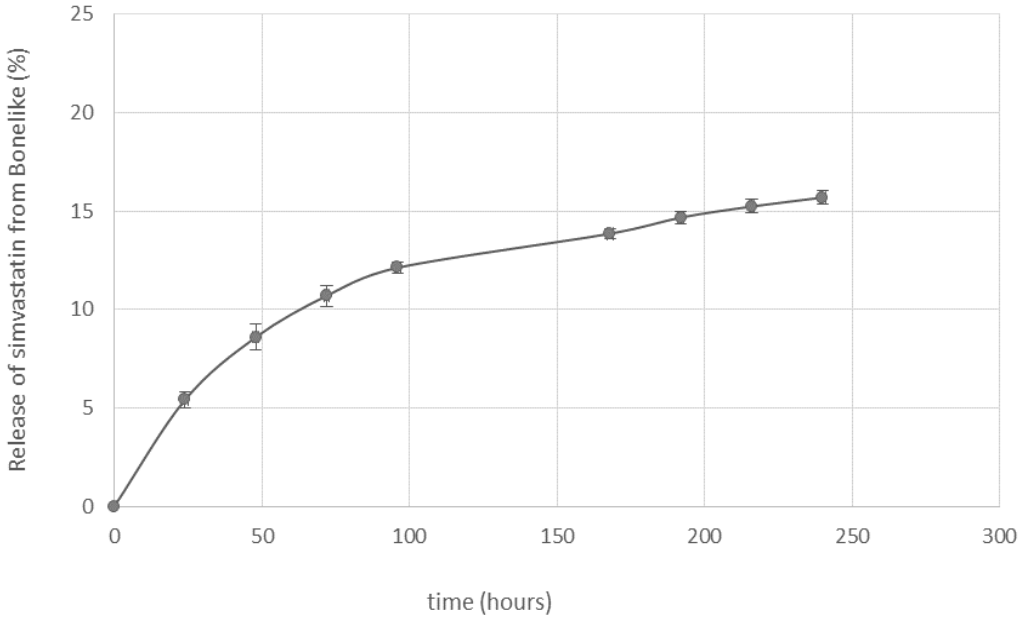

Figure 4.11 – Cumulative *in vitro* release of simvastatin from Bonelike.

The release pattern observed in the following days, showed that simvastatin is released gradually over time, after an initial burst from Bonelike, which goes in accordance to the published literature with similar materials [147]. It is important to mention that the scaffold, drug and medium quantities used in this test were the same as reported in literature [147], [159] and the results are in accordance. This lead us to assume that initially, the simvastatin that were present at the surface of Bonelike dissolves easily in the PBS until reaches the drug solubility limit. However, with the passage of time, the simvastatin that was present in the Bonelike surface was dissolved totally and only simvastatin entrapped inside Bonelike pores remained, what could explain the slow release. Therefore, Bonelike is capable of promoting a slow but constant release of simvastatin due to characteristics inherent to the material.

4.8 Incorporation of simvastatin in the nanogel

The possibility of enhancing simvastatin's solubility using dextrin nanoparticles as nanocarrier was investigated in this work. Therapeutic agents can either be physically entrapped into the polymeric matrix or covalently bound to the polymer backbone, being the physical drug entrapment the more often used loading method for drug delivery applications [131], and the one that was used in this work. Physical drug loading can be performed by incorporating the drug while producing the nanoparticles, or by incubating a concentrated drug solution with the already formed nanocarrier.

In this study, simvastatin was dissolved in a suitable solvent (ethanol) and exhibits absorption in the wavelength range from 200 to 255 nm, with a maximum absorption at 238 nm.

Gonçalves *et al* [138]. have successfully loaded dextrin nanoparticles with curcumin, a lipophilic molecule and have reported that the addition of curcumin dissolved in ethanol to water (to a final concentration of ethanol < 1%), leads to curcumin precipitation. The addition of curcumin to aqueous solutions of nanoparticles results in a bright yellow solution, what suggest the entrapment of curcumin, presumably into the hydrophobic domains within the nanoparticles [131]. While curcumin entrapment in the nanoparticles can be easily identified by the solutions with yellow colour, the simvastatin solutions are colorless. The dextrin nanoparticles in water originate a colloidal stable solution over 2 months; if the nanoparticles are centrifuged (<16000 rpm), they will not precipitate. Having this in mind, preliminary tests had place to determine if it was possible to load simvastatin in the nanoparticles. To aqueous nanoparticles solutions with diferent concentrations was added simvastatin dissolved in ethanol (to a final concentration of ethanol < 1%), centrifuged at 10000 rpm during 5 minutes. With nanoparticles solutions only a small white precipitate was formed at the bottom of the eppendorfs, while with the water control solutions all the simvastatin precipitated. This suggested the entrapment of simvastatin in the nanoparticles that was confirmed by UV spectra that reveal the same profile as the simvastatin dissolved in ethanol.

To evaluate entrapment efficiency, different parameters were tested, in particular the simvastatin and nanoparticles concentration and the encapsulation time. The results are presented in figure 4.13:

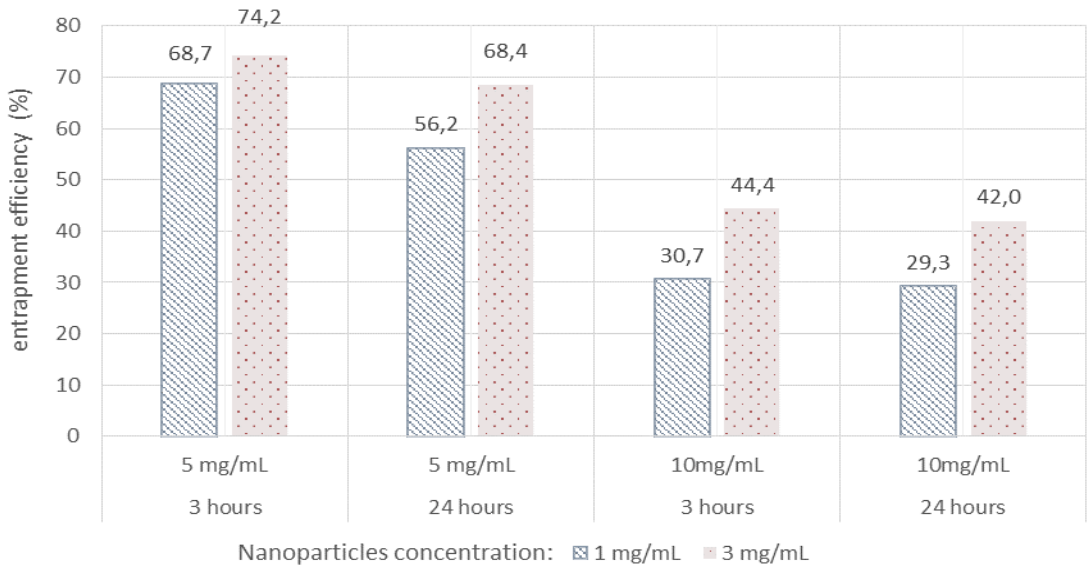

Figure 4.12 - Simvastatin loading into dextrin nanoparticles of different formulations varying the simvastatin (5 or 10 mg/mL), the nanoparticles (1 or 3 mg/mL) and time (3 or 24 hours).

As expected, there is an optimal proportion between drug and polymer that allows a better entrapment efficacy, which in this case was registered at 5 mg/mL of simvastatin and 3 mg/mL of dextrin nanoparticles, during 3 hours. Higher concentrations of simvastatin decrease the entrapment efficacy, as expected. At 3 hours, where the best results were found, 5mg/mL have efficacy of ~70-75%, while at 10mg/mL amounted to ~30-45%. Doubling the drug concentration reduce to half the entrapment efficacy. These findings indicate that 5mg/mL of simvastatin could be the maximum concentration limit for the incorporation of simvastatin in the dextrin nanoparticles. The nanoparticles are interesting drug delivery systems since they can control and sustain drug release at the target site, improving the therapeutic efficacy and reducing side effects [131]. In this work, the drug loading is relatively high and was achieved without chemical reactions; this is an important factor for preserving the drug activity [131], [138]. The polydispersity index (Pdl) is helpful in the characterization of the size distribution. Pdl-values close to 1 are indicative of heterogeneity [134]. The mean diameters (z-avg) of unloaded and simvastatin-loaded nanoparticles were found to be 20 nm (Pdl 0.452) and 28 nm (Pdl 0,615) for PBS solution, respectively. These are fairly high Pdl values, suggestive of significant polidispersity. This increase in size is in accordance with the published literature [138].

4.9 *In vitro* assay of simvastatin release from the nanogel

For the *in vitro* release of simvastatin from the dextrin nanoparticles, sink conditions were used. A drug release assay should use a sufficient volume of dissolution medium, which should be able to dissolve the expected amount of drug released from the sample. The ability of the medium to dissolve the expected amount of drug is known as a sink condition.

In this work, the soluble drug was quantified spectrophotometrically after centrifugation. This methodology is based on the fact that unentrapped simvastatin precipitates after centrifugation, as referred before. Only the entrapped simvastatin (0,1mM) in the nanoparticles is being quantified, since the sample was removed from inside the dialysis membrane.

A sustained release of simvastatin was observed (figure 4.14); After 1 and 3 hours, the fractions of simvastatin released to the PBS were respectively 26,1% and 43,7%.

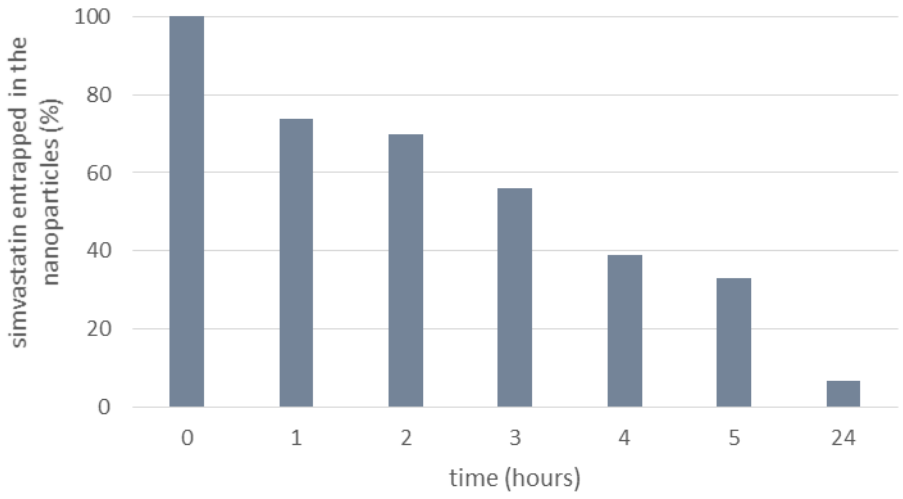

Figure 4.13 - In vitro simvastatin release from dextrin nanoparticles (1mg/mL).

The release profile without initial burst indicates the absence of simvastatin adsorbed on the surface of nanoparticles [191].The low size of the dextrin nanoparticles may explain the complete release of simvastatin in 24 hours, since drug release is affected by particle size. Drug associated with small particles would be at or near the nanoparticle surface, which leads to a faster drug release. Larger particles have larger cores, which allows more drug encapsulation per particle, providing a slower release [192]. Nevertheless, it is not expected that in an *in vivo* implant the release would occur in 24 hours. The *in vivo* injectable sample will have the nanoparticles inside the hydrogel matrix, which will prolong the release of simvastatin. Molinos *et al*. reported the release of the dextrin nanogel from the oDex-nanogel hydrogels. The nanogel was gradually release over time, paralleling the hydrogel degradation [105]. Therefore, it is expected that the release of simvastatin from the nanogel, follow the release of the nanogel from the hydrogel providing a steady and continuous release up to 1-2 weeks.

4.10 Materials sterilization

Being the injectable composed by different materials with very different properties, the sterilization procedures were made separately and then all materials were joined in aceptical and sterilized conditions. The sterilization process for the Bonelike and for the nanoparticles was already reported; the same methods were used in this work [49], [81], [131], [136].
Regarding the oDex hydrogel, some concerns arose about the reported sterilization process used in previous tests, where the hydrogel was sterilized by ethylene oxide [105]. The material has to be sterilized after the lyophilization process and before adding the reticulating agent. During this period, the material have a cotton-like texture and when sterilized by ethylene oxide, the gas enters to the material and effectively sterilize the hydrogel. However, after this process, the material has to rest during ten days and, more important, the reticulation time of the hydrogel increases. This indicate that the sterilization process is affecting the hydrogel matrix. In order to overcome this situation, other possibilities were studied, namely gamma radiation and ultraviolet radiation, but due to costs and time issues, only ultraviolet radiation efficacy was evaluated in this work. Samples of lyophilized hydrogel were immersed in αMEM to evaluate if the medium became cloudy or changed color due to bacterial growth. After four weeks, the medium remained with the same color and characteristics. More relevant, when UV sterilized samples of the hydrogel were reticulated, the gelation time was not altered, what allow to conclude that our material was successfully sterilized.

4.11 MTT assay

Simvastatin-loaded nanoparticles cytotoxicity was evaluated *in vitro*, using the 3-(4,5-dimethylthiazol-2-yl)-2,5-diphenyltetrazolium bromide (MTT) assay. The tetrazolium salt is widely used to quantify cytotoxicity, by colorimetry. The tetrazolium salts are metabolically reduced to highly coloured products, formazans. The colourless MTT is cleaved to formazan by the succinate-tetrazolium reductase system that belongs to the mitochondrial respiratory chain and is active only in viable cells [136].
In this study, mouse embryo fibroblasts 3T3 cells were used. Figure 4.16 depicts the MTT absorbance values obtained after 24 and 48 hours of incubation.

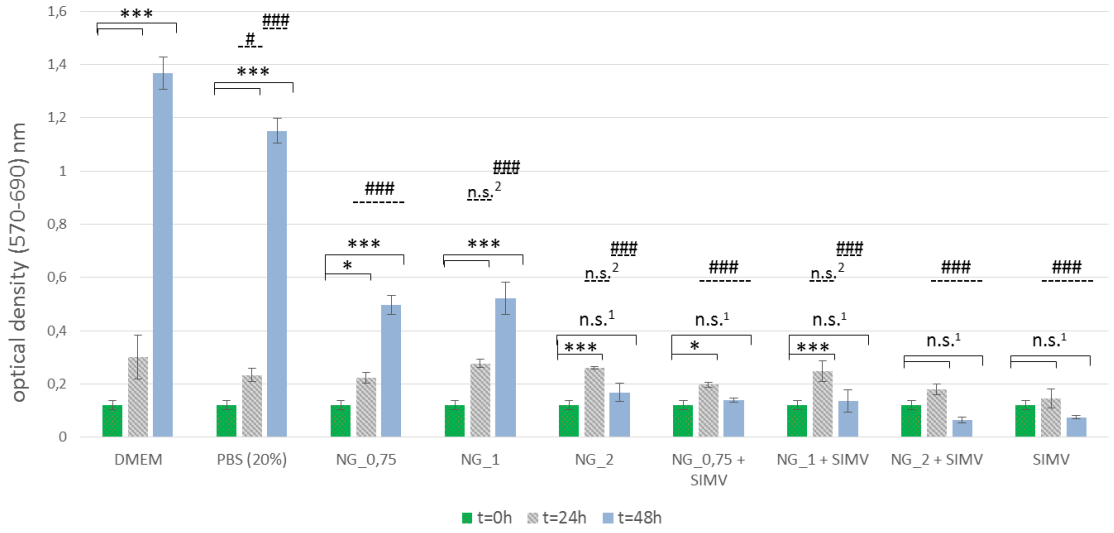

Figure 4.14 - Cells metabolic activity for different concentration of nanoparticles (0.75, 1 and 2 mg/mL), nanoparticles loaded with simvastatin and free simvastatin, assessed by MTT assay. Results presented as average ± SD (n=3). Statistical analysis were performed using a 2-way ANOVA. The comparison between diferent time points and t0 control are represented as n.s.[1]: non significant, $p>0.05$; *$p<0.05$; ***$p<0.001$. n.s.[2]: non significant, $p>0.05$; # $p<0.05$; ### $p<0.001$, represents each condition compared with the control (DMEM) at each timepoint (24 and 48 hours).

High concentrations of nanoparticles were tested, comparing with previous reports [136], [138]; this was due to the results of the tests of simvastatin incorporation in the nanoparticles, were 3 mg/mL registed the better results. However, to have a concentration of 3 mg/mL would be necessary to produce a sotck solution of nanoparticles at a concentration of 15 mg/mL, since the nanoparticles solutions were dissolved in cDMEM at 20% (v/v). This value was above the solubility limit of the material, so the highest concentration used in the cells was 2 mg/mL.

In the first 24 hours, the presence of nanoparticles and simvastatin-loaded nanoparticles does not affect cell metabolic activity. The cells showed an optical density similar to the control (t24h, untreated cells).

At 48 hours, the conditions with simvastatin loaded nanoparticles registered a low cell metabolic activity. This occurs due the release of simvastatin from the nanoparticles that happens during the first 24 hours. However the effects are not immediate, as can be seen in the first 24 hours of the condition with free simvastatin. Only at 48, the free simvastatin induced cell death. The nanoparticles at a concentration of 2mg/mL was not cytotoxic, but a cell proliferation inhibition can be observed at 48h. The simvastatin loaded nanoparticles (2mg/mL) induced cell death due to the joint action of the high nanoparticle concentration and simvastatin that was released for the medium. Although not statistically significant, existed biological differences in the conditions with simvastatin-loaded nanoparticles at 2mg/mL and free simvastatin where cell death at 48 hours occurred.

While the free simvastatin induced cell death and inhibited cell proliferation, the simvastatin loaded nanoparticles (0.75 and 1) did not induced cell death, comparing with the timepoint t0.

This showed the capacity of the nanogel to incorporated and produce a sustained release of the simvastatin, protecting the cells from the effects of the free simvastatin.
The overall results showed that the nanoparticles, at the concentrations studied, do not induced cell death. However, high concentrations of nanoparticles can constrain cell proliferation. In an *in vivo* application, it is expected that the results will be differents. While in the conditions tested the high concentration of nanoparticles inhibit cell proliferation, in the final injectable composite the nanoparticles will be within the hydrogel matrix, where they will have a slow release to the medium. In this case, the effects of high nanoparticles concentration and simvastatin will be attenuated.

4.12 *In vivo* tests

The *in vivo* tests are still in progress, so the results are not described in this work.

Chapter 5
Conclusions and Perspectives

The main purpose of the present work has been the development of an injectable bone substitute compose by a modified calcium phosphate (Bonelike) suspended in a dextrin hydrogel carrier. The possibility of use the injectable composite as a simvastatin carrier was also evaluated with different lines of investigation, namely with the incorporation in the Bonelike and in dextrin nanoparticles. The results obtained lead to the following main conclusions:
The composite system presented the capacity of being injected through a syringe and display gelation times suitable for the application in clinical environment.
Cryo-SEM analysis revealed that Bonelike granules are fully dispersed in the hydrogel matrix; the material produced is a three-dimensional, highly porous structure with interconnected porosity, displaying characteristic that will serve as scaffold for tissue growth.
The straightforward incorporation of simvastatin in the Bonelike and the slow but constant release of simvastatin to the medium makes the Bonelike an interesting simvastatin carrier, with similar results to the published literature for similar materials.
Taking advantage of nanotechnology in the drug delivery field, dextrin nanoparticles were used for improving simvastatin solubilisation and controlling its release profile. Despite the drug release occurs in a timeframe of 24 hours, it is expected that in the composite system this release is prolonged in time, up to 1-2 weeks.
Sterilization methods for the hydrogel was also addressed, and a successful method (ultraviolet radiation) that does not alter the reticulation time of the oDex hydrogels was found.
The evaluation of the cytotoxicity of the simvastatin loaded nanoparticles indicated the protective effect of the nanoparticles over the free simvastatin during 48 hours, and proved the effective release of simvastatin from the nanoparticles.
The use of injectable systems in bone tissue engineering is still in its early stages; however, the proposed system may constitute an advanced delivery system for simvastatin and a promising injectable composite material for bone regeneration.

The following goals are proposed for future work:

- Optimizing *in vitro* testing methodology for recreate similar conditions to the *in vivo* applications to extract more information about the behaviour of the composite system;
- Study the interaction between the scaffold material, its architecture and therapeutic agents, with the cells to fully understand how to regenerate engineered bone.

- Explore the incorporation of other drugs and micro or nanoparticles in the composite system;

References

[1] K. A. Hing, “Bone repair in the twenty-first century: biology, chemistry or engineering?,” *Philos. Trans. A. Math. Phys. Eng. Sci.*, vol. 362, pp. 2821–2850, 2004.

[2] P. A. Downey and M. I. Siegel, “Bone biology and the clinical implications for osteoporosis,” *Phys Ther*, vol. 86, pp. 77–91, 2006.

[3] M. J. Olszta, X. Cheng, S. S. Jee, R. Kumar, Y. Y. Kim, M. J. Kaufman, E. P. Douglas, and L. B. Gower, “Bone structure and formation: A new perspective,” *Materials Science and Engineering R: Reports*, vol. 58. pp. 77–116, 2007.

[4] R. Seeley, T. D. Stephens, and P. Tate, “Anatomy and Physiology.,” *Br. Med. J.*, vol. 1, pp. 805–806, 2007.

[5] A. S. Mistry and A. G. Mikos, “Tissue engineering strategies for bone regeneration.,” *Adv. Biochem. Eng. Biotechnol.*, vol. 94, pp. 1–22, 2005.

[6] G. S. Travlos, “Normal structure, function, and histology of the bone marrow.,” *Toxicol. Pathol.*, vol. 34, pp. 548–565, 2006.

[7] N. PERMATA, “Understanding Compact Bone,” *Sridianti.com*, 2015. [Online]. Available: http://www.sridianti.com/pengertian-tulang-kompak.html. [Accessed: 03-Apr-2015].

[8] A. J. Salgado, O. P. Coutinho, and R. L. Reis, “Bone tissue engineering: State of the art and future trends,” *Macromolecular Bioscience*, vol. 4. pp. 743–765, 2004.

[9] S. Lou Bonnick, *Bone Densitometry in Clinical Practice*. 2010.

[10] K. A. Athanasiou, C. Zhu, D. R. Lanctot, C. M. Agrawal, and X. Wang, “Fundamentals of biomechanics in tissue engineering of bone.,” *Tissue Eng.*, vol. 6, pp. 361–381, 2000.

[11] H. I. Roach, “Why does bone matrix contain non-collagenous proteins? The possible roles of osteocalcin, osteonectin, osteopontin and bone sialoprotein in bone mineralisation and resorption.,” *Cell Biol. Int.*, vol. 18, pp. 617–628, 1994.

[12] B. Alberts, A. Johnson, J. Lewis, M. Raff, K. Roberts, and P. Walter, *Molecular Biology of the Cell*. 2002.

[13] C. B. Khatiwala, S. R. Peyton, and A. J. Putnam, “Intrinsic mechanical properties of the extracellular matrix affect the behavior of pre-osteoblastic MC3T3-E1 cells.,” *Am. J. Physiol. Cell Physiol.*, vol. 290, pp. C1640–C1650, 2006.

[14] M. Simian, Y. Hirai, M. Navre, Z. Werb, A. Lochter, and M. J. Bissell, “The interplay of matrix metalloproteinases, morphogens and growth factors is necessary for branching of mammary epithelial cells.,” *Development*, vol. 128, pp. 3117–3131, 2001.

[15] B. Clarke, “Normal bone anatomy and physiology.,” *Clin. J. Am. Soc. Nephrol.*, vol. 3 Suppl 3, pp. S131–9, 2008.

[16] N. Takahashi, N. Udagawa, Y. Kobayashi, M. Takami, and T. Suda, *Principles of Bone Biology*. 2008.

[17] P. Grabowski, “Physiology of bone,” *Endocrine Development*, vol. 16. pp. 32–48, 2009.

[18] P. A. Hill, “Bone remodelling,” *Br. J. Orthod.*, vol. 25, pp. 101–107, 1998.

[19] D. J. Hadjidakis and I. I. Androulakis, “Bone remodeling.,” *Ann. N. Y. Acad. Sci.*, vol. 1092, pp. 385–96, Dec. 2006.

[20] N. Rucci, “Molecular biology of bone remodelling,” pp. 49–56, 2008.

[21] Osteocord, “Bone remodelling,” 2005. [Online]. Available: http://www.york.ac.uk/res/bonefromblood/background/boneremodelling.html. [Accessed: 13-Mar-2015].

[22] R. Marsell and T. A. Einhorn, “Emerging bone healing therapies.,” *J. Orthop. Trauma*, vol. 24 Suppl 1, pp. S4–S8, 2010.

[23] R. Marsell and T. A. Einhorn, “The biology of fracture healing,” *Injury*, vol. 42. pp. 551–555, 2011.

[24] B. Biology, “Bone Remodeling and Repair,” 2015. [Online]. Available: https://www.boundless.com/biology/textbooks/boundless-biology-textbook/the-musculoskeletal-system-38/bone-216/bone-remodeling-and-repair-819-12062/. [Accessed: 11-Jun-2015].

[25] I. H. Kalfas, “Principles of bone healing.,” *Neurosurg. Focus*, vol. 10, p. E1, 2001.

[26] L. Marzona and B. Pavolini, “Play and players in bone fracture healing match,” *Clinical Cases in Mineral and Bone Metabolism*, vol. 6. pp. 159–162, 2009.

[27] B. D. Ratner, A. S. Hoffman, F. J. Schoen, and J. E. Lemons, *Biomaterials Science: An Introduction to Materials in Medicine*, vol. 22. 2004, p. 851.

[28] N. Huebsch and D. J. Mooney, “Inspiration and application in the evolution of biomaterials.,” *Nature*, vol. 462, pp. 426–432, 2009.

[29] N. R. Patel and P. P. Gohil, “A Review on Biomaterials : Scope , Applications & Human Anatomy Significance,” vol. 2, no. 4, 2012.

[30] P. V Giannoudis, H. Dinopoulos, and E. Tsiridis, “Bone substitutes: an update.,” *Injury*, vol. 36 Suppl 3, pp. S20–S27, 2005.

[31] W. R. Moore, S. E. Graves, and G. I. Bain, “Synthetic bone graft substitutes.,” *ANZ J. Surg.*, vol. 71, pp. 354–361, 2001.

[32] J. C. Minichetti, J. C. D’Amore, A. Y. J. Hong, and D. B. Cleveland, *Human histologic analysis of mineralized bone allograft (Puros) placement before implant surgery.*, vol. 30. 2004, pp. 74–82.

[33] D. A. Dennis and L. R. Little, “The structural allograft composite in revision total knee arthroplasty.,” *Orthopedics*, vol. 28, pp. 1005–1007, 2005.

[34] CDC, “Infection Control - Centers for Disease Control and Prevention (CDC),” 2013. [Online]. Available: http://www.cdc.gov/oralhealth/infectioncontrol/faq/allografts.htm.

[35] G. Zimmermann and A. Moghaddam, “Allograft bone matrix versus synthetic bone graft substitutes,” *Injury*, vol. 42, 2011.

[36] A. S. Brydone, D. Meek, and S. Maclaine, “Bone grafting, orthopaedic biomaterials, and the clinical need for bone engineering.,” *Proc. Inst. Mech. Eng. H.*, vol. 224, pp. 1329–1343, 2010.

[37] R. N. Pierson, “Antibody-mediated xenograft injury: Mechanisms and protective strategies,” *Transpl. Immunol.*, vol. 21, pp. 65–69, 2009.

[38] D. I. Ilan and A. L. Ladd, “Bone graft substitutes,” *Oper. Tech. Plast. Reconstr. Surg.*, vol. 9, pp. 151–160, 2002.

[39] GlobalData, “Bone Grafts and Substitutes - Global Analysis and Market Forecasts.” [Online]. Available: http://healthcare.globaldata.com/media-center/press-releases/medical-devices/bone-grafts-and-substitutes-market-bending-towards-steady-growth-by-2020-says-globaldata.

[40] S. V. Dorozhkin, “A detailed history of calcium orthophosphates from 1770s till 1950,” *Materials Science and Engineering C*, vol. 33. pp. 3085–3110, 2013.

[41] S. V. Dorozhkin, “Amorphous Calcium Orthophosphates: Nature, Chemistry and Biomedical Applications,” *Int. J. Mater. Chem.*, vol. 2, no. 1, pp. 19–46, Aug. 2012.

[42] S. V. Dorozhkin, “Calcium orthophosphates: occurrence, properties, biomineralization, pathological calcification and biomimetic applications.,” *Biomatter*, vol. 1. pp. 121–164, 2011.

[43] J. Keating and M. McQueen, “Substitutes for autologous bone graft in orthopaedic trauma.,” *J Bone Jt. Surg Br*, vol. 83, p. 777.

[44] C. M. Kelly, R. M. Wilkins, S. Gitelis, C. Hartjen, J. T. Watson, and P. T. Kim, “The use of a surgical grade calcium sulfate as a bone graft substitute: results of a multicenter trial.,” 2001.

[45] K. L. Low, S. H. Tan, S. H. S. Zein, J. A. Roether, V. Mouriño, and A. R. Boccaccini, “Calcium phosphate-based composites as injectable bone substitute materials,” *Journal of Biomedical Materials Research - Part B Applied Biomaterials*, vol. 94. pp. 273–286, 2010.

[46] T. Albrektsson and C. Johansson, “Osteoinduction, osteoconduction and osseointegration,” *Eur. Spine J.*, vol. 10, 2001.

[47] R. R. Betz, “Limitations of autograft and allograft: new synthetic solutions.,” *Orthopedics*, vol. 25, pp. s561–s570, 2002.

[48] M. Gutierres, M. A. Lopes, N. Sooraj Hussain, A. F. Lemos, J. M. F. Ferreira, A. Afonso, A. T. Cabral, L. Almeida, and J. D. Santos, “Bone ingrowth in macroporous Bonelike® for orthopaedic applications,” *Acta Biomater.*, vol. 4, pp. 370–377, 2008.

[49] M. Gutierres, N. S. Hussain, A. Afonso, L. Almeida, T. Cabral, M. A. Lopes, and J. D. Santos, “Biological Behaviour of Bonelike ® Graft Implanted in the Tibia of Humans,” vol. 286, pp. 1041–1044, 2005.

[50] F. Duarte, J. D. Santos, and A. Afonso, “Medical applications of Bonelike in Maxillofacial Surgery,” vol. 456, pp. 370–373, 2004.

[51] J. V. Lobato, N. Sooraj Hussain, C. M. Botelho, A. C. Maurício, J. M. Lobato, M. A. Lopes, A. Afonso, N. Ali, and J. D. Santos, “Titanium dental implants coated with Bonelike®: Clinical case report,” *Thin Solid Films*, vol. 515, pp. 279–284, 2006.

[52] J. V. Lobato, N. S. Hussain, M. A. Lopes, J. M. Lobato, and A. C. Maurício, “Clinical applications of Titanium dental implants coated with glass-reinforced Hydroxyapatite composite (Bonelike®).,” *Int. J. Nanomanuf.*, vol. 1–2, no. 2, pp. 135–148, 2008.

[53] J. Yao and A. M. Ho, “Bone Graft Substitutes in the Treatment of Distal Radius and Upper Limb Injuries,” *Oper. Tech. Orthop.*, vol. 19, pp. 77–87, 2009.

[54] A. Beswick and A. W. Blom, “Bone graft substitutes in hip revision surgery: A comprehensive overview,” *Injury*, vol. 42. 2011.

[55] E. D. Zanotto, “The applicability of the general theory of phase transformations to glass crystallization,” *Thermochim. Acta*, vol. 280–281, pp. 73–82, 1996.

[56] P. D. Sarkisov, N. Y. Mikhailenko, and L. A. Orlova, “Glass ceramic materials in the context of contemporary material science,” *Glas. Ceram. (English Transl. Steklo i Keramika)*, vol. 60, pp. 261–265, 2003.

[57] P. W. McMillan, “The crystallisation of glasses.,” *J. Non. Cryst. Solids*, vol. 52, no. 1–3, pp. 67–76, 1982.

[58] P. Ducheyne and Q. Qiu, “Bioactive ceramics: The effect of surface reactivity on bone formation and bone cell function,” *Biomaterials*, vol. 20. pp. 2287–2303, 1999.

[59] L. L. Hench, “Bioceramics,” *J. Am. Ceram. Soc.*, vol. 81, pp. 1705–1728, 1998.

[60] A. W. Blayney, J. P. Bebear, K. R. Williams, and M. Portmann, “Ceravital in ossiculoplasty: experimental studies and early clinical results.,” 1986.

[61] T. Kokubo, “Bioactive glass ceramics: properties and applications.,” *Biomaterials*, vol. 12, pp. 155–163, 1991.

[62] S. Yoshii, M. Oka, T. Yamamuro, K. Ikeda, and H. Murakami, “Acetabular augmentation using a glass-ceramic block: 3 patients followed 3-4 years.,” *Acta Orthop. Scand.*, vol. 71, pp. 580–584, 2000.

[63] M. B. Hall, H. R. Stanley, C. King, F. Colaizzi, S. D., and L. L. Hench, “Early clinical trials of 45S5 bioglass for endosseous alveolar ridge maintenance implants,” in *Tissue integration in oral and maxillo-facial reconstruction*, 1986, pp. 413–417.

[64] S. Yilmaz, E. Efeoğlu, and A. R. Kiliç, “Alveolar ridge reconstruction and/or preservation using root form bioglass cones.,” 1998.

[65] W. R. Lacefield and L. L. Hench, “The bonding of Bioglass to a cobalt-chromium surgical implant alloy.,” *Biomaterials*, vol. 7, pp. 104–108, 1986.

[66] S. Asano, K. Kaneda, S. Satoh, K. Abumi, T. Hashimoto, and M. Fujiya, *Reconstruction of an iliac crest defect with a bioactive ceramic prosthesis.*, vol. 3. 1994, pp. 39–44.

[67] L. L. Hench, “Biomaterials: A forecast for the future,” in *Biomaterials*, 1998, vol. 19, pp. 1419–1423.

[68] K. C. Dee, D. A. Puleo, R. Bizios, C. J. Wiley, and D. Ph, “Tissue- Biomaterial Interactions An Introduction To Tissue- Biomaterial Interactions,” *New York*, vol. 4, pp. 89–99, 2002.

[69] C. S. Cutter and B. J. Mehrara, “Bone grafts and substitutes.,” *J. Long. Term. Eff. Med. Implants*, vol. 16, pp. 249–260, 2006.

[70] M. Ceramics and V. A. Dubok, “BIOCERAMICS - YESTERDAY, TODAY, TOMORROW,” *Powder Metall. Met. Ceram.*, vol. 39, pp. 381–394, 2001.

[71] L. L. Hench, “Bioceramics: From Concept to Clinic,” *J. Am. Ceram. Soc.*, vol. 74, pp. 1487–1510, 1991.

[72] T. Nakamura, T. Yamamuro, S. Higashi, T. Kokubo, and S. Itoo, “A new glass-ceramic for bone replacement: Evaluation of its bonding to bone tissue,” *J. Biomed. Mater. Res.*, vol. 19, pp. 685–698, 1985.

[73] J. Lu, A. Gallur, B. Flautre, K. Anselme, M. Descamps, B. Thierry, and P. Hardouin, “Comparative study of tissue reactions to calcium phosphate ceramics among cancellous, cortical, and medullar bone sites in rabbits.,” *J Biomed Mater Res*, vol. 42, pp. 357–367, 1998.

[74] A. M. Gatti and D. Zaffe, “Bioactive glasses and chemical bond,” *Biomaterials*, vol. 13, pp. 97–107, 1992.

[75] D. Knaack, M. E. P. Goad, M. Aiolova, C. Rey, A. Tofighi, P. Chakravarthy, and D. D. Lee, “Resorbable calcium phosphate bone substitute,” *J. Biomed. Mater. Res.*, vol. 43, pp. 399–409, 1998.

[76] R. Z. LeGeros, “Biodegradation and bioresorption of calcium phosphate ceramics.,” *Clin. Mater.*, vol. 14, pp. 65–88, 1993.

[77] J. D. Santos, G. W. Hastings, and J. C. Knowles, “Sintered hydroxyapatite compositions and method for the preparation thereof,” WO 2000068164 A1, 1999.

[78] M. Gutierres, N. Sooraj Hussain, M. A. Lopes, A. Afonso, A. T. Cabral, L. Almeida, and J. D. Santos, “Histological and Scanning Electron Microscopy Analyses of Bone/Implant Interface Using the Novel Bonelike Synthetic Bone Graft,” *J. Orthop. Res.*, 2006.

[79] N. H. Sooraj, M. A. Lopes, A. C. Mauricio, and J. D. Santos, “Bonelike® Graft for Bone Regenerative Applications,” *Surf. Eng. Biomed. Surg. Devices*, vol. 13, pp. 477–512, 2007.

[80] J. Torres, M. Gutierres, M. A. Lopes, J. D. Santos, A. T. Cabral, R. Pinto, and C. van Eck, “Bone Marrow Stem Cells Added to a Hydroxyapatite Scaffold Result in Better Outcomes after Surgical Treatment of Intertrochanteric Hip Fractures,” *Biomed Res. Int.*, 2014.

[81] R. C. Sousa, J. V Lobato, A. C. Maurício, N. S. Hussain, C. M. Botelho, M. A. Lopes, and J. D. Santos, "A clinical report of bone regeneration in maxillofacial surgery using bonelike synthetic bone graft.," 2008.

[82] S. Larsson and G. Hannink, "Injectable bone-graft substitutes: Current products, their characteristics and indications, and new developments," *Injury*, vol. 42, 2011.

[83] M. Bohner, "Design of ceramic-based cements and putties for bone graft substitution," *Eur. Cells Mater.*, vol. 20, pp. 1–12, 2010.

[84] American Academy of Orthopaedic Surgeons, "Summary of typical bone-graft substitutes that are commercially available - 2010," 2010.

[85] A. Gutowska, B. Jeong, and M. Jasionowski, "Injectable gels for tissue engineering," *Anat. Rec.*, vol. 263, pp. 342–349, 2001.

[86] R. T. Tran, D. Gyawali, P. Nair, and J. Yang, "Chapter 14: Biodegradable Injectable Systems for Bone Tissue Engineering," in *A Handbook of Applied Biopolymer Technology: Synthesis, Degradation and Applications*, vol. 12, 2012.

[87] G. Schmidmaier, P. Schwabe, B. Wildemann, and N. P. Haas, "Use of bone morphogenetic proteins for treatment of non-unions and future perspectives," *Injury*, vol. 38, no. 4, pp. 35–41, 2007.

[88] A. S. Hickey and N. A. Peppas, "Mesh size and diffusive characteristics of semicrystalline poly(vinyl alcohol) membranes prepared by freezing/thawing techniques," *J. Memb. Sci.*, vol. 107, pp. 229–237, 1995.

[89] N. Kashyap, N. Kumar, and M. N. Kumar, "Hydrogels for pharmaceutical and biomedical applications.," *Crit Rev Ther Drug Carr. Syst*, vol. 22, pp. 107–149, 2005.

[90] N. A. Peppas, J. Z. Hilt, A. Khademhosseini, and R. Langer, "Hydrogels in biology and medicine: From molecular principles to bionanotechnology," *Advanced Materials*, vol. 18. pp. 1345–1360, 2006.

[91] A. M. Lowman and N. A. Peppas, "Analysis of the complexation/ decomplexation phenomena in graft copolymer networks.," *Macromolecules*, vol. 30, pp. 4959–4965, 1997.

[92] A. M. Lowman and N. A. Peppas, "Hydrogels.," *Encyclopedia of Controlled Drug Delivery*. pp. 397–418, 1999.

[93] X. Jia and K. L. Kiick, "Hybrid multicomponent hydrogels for tissue engineering," *Macromolecular Bioscience*, vol. 9. pp. 140–156, 2009.

[94] N. A. Peppas, Y. Huang, M. Torres-Lugo, J. H. Ward, and J. Zhang, "Physicochemical foundations and structural design of hydrogels in medicine and biology.," *Annu. Rev. Biomed. Eng.*, vol. 2, pp. 9–29, 2000.

[95] M. W. Tibbitt and K. S. Anseth, "Hydrogels as extracellular matrix mimics for 3D cell culture," *Biotechnology and Bioengineering*, vol. 103. pp. 655–663, 2009.

[96] J. L. Long and R. T. Tranquillo, "Elastic fiber production in cardiovascular tissue-equivalents," *Matrix Biol.*, vol. 22, pp. 339–350, 2003.

[97] P. S. Robinson, S. L. Johnson, M. C. Evans, V. H. Barocas, and R. T. Tranquillo, "Functional tissue-engineered valves from cell-remodeled fibrin with commissural alignment of cell-produced collagen.," *Tissue Eng. Part A*, vol. 14, pp. 83–95, 2008.

[98] R. Sbarbati Delguerra, M. G. Cascone, D. Ricci, S. Martinoia, M. T. Parodi, A. Ahluwalia, J. A. Van Mourik, and M. Grattarola, "Optimization of the interaction between ethylene-vinyl alcohol copolymers and human endothelial cells," *J. Mater. Sci. Mater. Med.*, vol. 7, pp. 8–12, 1996.

[99] C. J. Kirkpatrick, "A critical view of current and proposed methodologies for biocompatibility testing: cytotoxicity in vitro," *Regul. Aff.*, vol. 4, pp. 13–32, 1992.

[100] W. Y. Su, Y. C. Chen, and F. H. Lin, "Injectable oxidized hyaluronic acid/adipic acid dihydrazide hydrogel for nucleus pulposus regeneration," *Acta Biomater.*, vol. 6, pp. 3044–3055, 2010.

[101] Y. teng Wei, F. zhai Cui, and W. ming Tian, "Fabrication and characterization of hyaluronic-acid-based antigen sensitive degradable hydrogel," *Front. Mater. Sci. China*, vol. 3, pp. 353–358, 2009.

[102] F. C. McGillicuddy, I. Lynch, Y. A. Rochev, M. Burke, K. A. Dawson, W. M. Gallagher, and A. K. Keenan, "Novel 'plum pudding' gels as potential drug-eluting stent coatings: Controlled release of fluvastatin," *J. Biomed. Mater. Res. - Part A*, vol. 79, pp. 923–933, 2006.

[103] I. Lynch and K. A. Dawson, "Synthesis and Characterization of an Extremely Versatile Structural Motif Called the 'Plum-Pudding' Gel," *J Phys Chem B*, vol. 107, pp. 9629–9637, 2003.

[104] I. Lynch, P. De Gregorio, and K. A. Dawson, "Simultaneous release of hydrophobic and cationic solutes from thin-film 'plum-pudding' gels: A multifunctional platform for surface drug delivery?," *J. Phys. Chem. B*, vol. 109, pp. 6257–6261, 2005.

[105] M. Molinos, V. Carvalho, D. M. Silva, and F. M. Gama, "Development of a hybrid dextrin hydrogel encapsulating dextrin nanogel as protein delivery system," *Biomacromolecules*, vol. 13, pp. 517–527, 2012.

[106] F. Munarin, S. G. Guerreiro, M. A. Grellier, M. C. Tanzi, M. A. Barbosa, P. Petrini, and P. L. Granja, "Pectin-based injectable biomaterials for bone tissue engineering," *Biomacromolecules*, vol. 12, pp. 568–577, 2011.

[107] J. Carvalho, C. Gonçalves, A. M. Gil, and F. M. Gama, "Production and characterization of a new dextrin based hydrogel," *Eur. Polym. J.*, vol. 43, pp. 3050–3059, 2007.

[108] T. Coviello, P. Matricardi, C. Marianecci, and F. Alhaique, "Polysaccharide hydrogels for modified release formulations," *Journal of Controlled Release*, vol. 119. pp. 5–24, 2007.

[109] T. C. Flanagan, B. Wilkins, A. Black, S. Jockenhoevel, T. J. Smith, and A. S. Pandit, "A collagen-glycosaminoglycan co-culture model for heart valve tissue engineering applications," *Biomaterials*, vol. 27, pp. 2233–2246, 2006.

[110] S. In Jeong, S. Y. Kim, S. K. Cho, M. S. Chong, K. S. Kim, H. Kim, S. B. Lee, and Y. M. Lee, "Tissue-engineered vascular grafts composed of marine collagen and PLGA fibers using pulsatile perfusion bioreactors," *Biomaterials*, vol. 28, pp. 1115–1122, 2007.

[111] B. Liu, S. X. Cai, K. W. Ma, Z. L. Xu, X. Z. Dai, L. Yang, C. Lin, X. B. Fu, K. L. Sung, and X. K. Li, "Fabrication of a PLGA-collagen peripheral nerve scaffold and investigation of

its sustained release property in vitro," *J. Mater. Sci. Mater. Med.*, vol. 19, pp. 1127–1132, 2008.

[112] S. Zhong, W. E. Teo, X. Zhu, R. Beuerman, S. Ramakrishna, and L. Y. Yung, "Formation of collagenglycosaminoglycan blended nanofibrous scaffolds and their biological properties.," *Biomacromolecules*, vol. 6, pp. 2998–3004, 2005.

[113] G. W. Bos, J. J. L. Jacobs, J. W. Koten, S. Van Tomme, T. Veldhuis, C. F. Van Nostrum, W. Den Otter, and W. E. Hennink, "In situ crosslinked biodegradable hydrogels loaded with IL-2 are effective tools for local IL-2 therapy," *Eur. J. Pharm. Sci.*, vol. 21, pp. 561–567, 2004.

[114] S. G. Lévesque and M. S. Shoichet, "Synthesis of cell-adhesive dextran hydrogels and macroporous scaffolds," *Biomaterials*, vol. 27, pp. 5277–5285, 2006.

[115] S. Kim and S. B. Lee, "Soluble expression of archaeal proteins in Escherichia coli by using fusion-partners," *Protein Expr. Purif.*, vol. 62, pp. 116–119, 2008.

[116] C. K. Kuo and P. X. Ma, "Ionically crosslinked alginate hydrogels as scaffolds for tissue engineering: Part 1. Structure, gelation rate and mechanical properties," *Biomaterials*, vol. 22, pp. 511–521, 2001.

[117] P. Eiselt, J. Yeh, R. K. Latvala, L. D. Shea, and D. J. Mooney, "Porous carriers for biomedical applications based on alginate hydrogels," *Biomaterials*, vol. 21, pp. 1921–1927, 2000.

[118] L. N. Novikova, A. Mosahebi, M. Wiberg, G. Terenghi, J. O. Kellerth, and L. N. Novikov, "Alginate hydrogel and matrigel as potential cell carriers for neurotransplantation," *J. Biomed. Mater. Res. - Part A*, vol. 77, pp. 242–252, 2006.

[119] M. Veerapandian and K. Yun, "The state of the art in biomaterials as nanobiopharmaceuticals," *Digest Journal of Nanomaterials and Biostructures*, vol. 4. pp. 243–262, 2009.

[120] C. T. Schwall and I. A. Banerjee, "Micro- and nanoscale hydrogel systems for drug delivery and tissue engineering," *Materials*, vol. 2. pp. 577–612, 2009.

[121] D. R. Nisbet, K. E. Crompton, S. D. Hamilton, S. Shirakawa, R. J. Prankerd, D. I. Finkelstein, M. K. Horne, and J. S. Forsythe, "Morphology and gelation of thermosensitive xyloglucan hydrogels," *Biophys. Chem.*, vol. 121, pp. 14–20, 2006.

[122] D. M. Lazarus, "Adhesives based on starch," in *Adhesion 7*, 1983, pp. 197–219.

[123] D. Hreczuk-Hirst, D. Chicco, L. German, and R. Duncan, "Dextrins as potential carriers for drug targeting: Tailored rates of dextrin degradation by introduction of pendant groups," *Int. J. Pharm.*, vol. 230, pp. 57–66, 2001.

[124] P. Tomasik, S. Wiejak, and M. Pałasiński, "The Thermal Decomposition of Carbohydrates. Part II. The Decomposition of Starch," in *Advances in Carbohydrate Chemistry and Biochemistry*, vol. 47, 1989, pp. 279–343.

[125] F. M. Gama and M. C. Molinos, "Dextrin hydrogel for biomedical applications," WO2011070529 A2, 2011.

[126] K. B. Hosie, D. J. Kerr, J. A. Gilbert, M. Downes, G. Lakin, G. Pemberton, K. Timms, A. Young, and A. Stanley, "A pilot study of adjuvant intraperitoneal 5-fluorouracil using 4% icodextrin as a novel carrier solution," *Eur. J. Surg. Oncol.*, vol. 29, pp. 254–260, 2003.

[127] J. E. Frampton and G. L. Plosker, “Icodextrin: A review of its use in peritoneal dialysis,” *Drugs*, vol. 63. pp. 2079–2105, 2003.

[128] J. Hardwicke, R. Moseley, P. Stephens, K. Harding, R. Duncan, and D. W. Thomas, “Bioresponsive dextrin-rhEGF conjugates: In vitro evaluation in models relevant to its proposed use as a treatment for chronic wounds,” *Mol. Pharm.*, vol. 7, pp. 699–707, 2010.

[129] T. Asai, T. Hayashi, S. Hamajima, A. Mieki, H. Kataoka, and T. Kawai, “Development of Bone Filling Material made from the Dextrin Complex,” *Am. Assoc. Dent. Res.*, 2009.

[130] J. Carvalho, S. Moreira, J. Maia, and F. M. Gama, “Characterization of dextrin-based hydrogels: Rheology, biocompatibility, and degradation,” *J. Biomed. Mater. Res. - Part A*, vol. 93, pp. 389–399, 2010.

[131] C. Gonçalves, P. Pereira, and M. Gama, “Self-assembled hydrogel nanoparticles for drug delivery applications,” *Materials*, vol. 3. pp. 1420–1460, 2010.

[132] C. Gonçalves, “Development of self-assembled dextrin nanogels,” Universidade do Minho, 2010.

[133] M. Hans, K. Shimoni, D. Danino, S. J. Siégel, and A. Lowman, “Synthesis and characterization of mPEG-PLA prodrug micelles,” *Biomacromolecules*, vol. 6, pp. 2708–2717, 2005.

[134] C. Gonçalves, J. A. Martins, and F. M. Gama, “Self-assembled nanoparticles of dextrin substituted with hexadecanethiol,” *Biomacromolecules*, vol. 8, pp. 392–398, 2007.

[135] C. Gonçalves and F. M. Gama, “Characterization of the self-assembly process of hydrophobically modified dextrin,” *Eur. Polym. J.*, vol. 44, pp. 3529–3534, 2008.

[136] C. Gonçalves, E. Torrado, T. Martins, P. Pereira, J. Pedrosa, and M. Gama, “Dextrin nanoparticles: Studies on the interaction with murine macrophages and blood clearance,” *Colloids Surfaces B Biointerfaces*, vol. 75, pp. 483–489, 2010.

[137] C. Gonçalves, M. F. M. Ferreira, A. C. Santos, M. I. M. Prata, C. F. G. C. Geraldes, J. A. Martins, and F. M. Gama, “Studies on the biodistribution of dextrin nanoparticles.,” *Nanotechnology*, vol. 21, p. 295103, 2010.

[138] C. Gonçalves, P. Pereira, P. Schellenberg, P. J. Coutinho, and F. M. Gama, “Self-Assembled Dextrin Nanogel as Curcumin Delivery System,” *J. Biomater. Nanobiotechnol.*, vol. 3, pp. 178–184, 2012.

[139] J. Montero, G. Manzano, and A. Albaladejo, “The role of topical simvastatin on bone regeneration : A systematic review,” *J Clin Exp Dent*, vol. 6, no. 3, pp. 286–290, 2014.

[140] M. R. Urist, R. J. DeLange, and G. A. Finerman, “Bone cell differentiation and growth factors,” *Science (80-.).*, vol. 220, pp. 680–686, 1983.

[141] D. Chen, M. Zhao, and G. R. Mundy, “Bone morphogenetic proteins.,” *Growth Factors*, vol. 22, pp. 233–241, 2004.

[142] P. J. Marie, F. Debiais, and E. Haÿ, “Regulation of human cranial osteoblast phenotype by FGF-2, FGFR-2 and BMP-2 signaling,” *Histology and Histopathology*, vol. 17. pp. 877–885, 2002.

[143] P. J. Boyne, S. Salina, A. Nakamura, F. Audia, and S. Shabahang, “Bone regeneration using rhBMP-2 induction in hemimandibulectomy type defects of elderly sub-human primates,” *Cell Tissue Bank.*, vol. 7, pp. 1–10, 2006.

[144] A. C. Killeen, P. A. Rakes, M. J. Schmid, Y. Zhang, N. Narayana, D. B. Marx, J. B. Payne, D. Wang, and R. A. Reinhardt, “Impact of Local and Systemic Alendronate on Simvastatin-Induced New Bone Around Periodontal Defects,” *Journal of Periodontology*. pp. 1–11, 2012.

[145] S. Srisubut, A. Teerakapong, T. Vattraphodes, and S. Taweechaisupapong, “Effect of local delivery of alendronate on bone formation in bioactive glass grafting in rats,” *Oral Surgery, Oral Med. Oral Pathol. Oral Radiol. Endodontology*, vol. 104, 2007.

[146] S. Chen, J. Y. Yang, S. Y. Zhang, L. Feng, and J. Ren, “Effects of simvastatin gel on bone regeneration in alveolar defects in miniature pigs,” *Chin. Med. J. (Engl).*, vol. 124, pp. 3953–3958, 2011.

[147] S. Gao, M. Shiota, M. Fujii, K. Chen, M. Shimogishi, M. Sato, and S. Kasugai, “Combination of simvastatin and hydroxyapatite fiber induces bone augmentation,” *Open J. Regen. Med.*, vol. 02, no. 03, pp. 53–60, 2013.

[148] G. Mundy, R. Garrett, S. Harris, J. Chan, D. Chen, G. Rossini, B. Boyce, M. Zhao, and G. Gutierrez, “Stimulation of bone formation in vitro and in rodents by statins.,” *Science*, vol. 286, pp. 1946–1949, 1999.

[149] S. B. Jadhav and G. K. Jain, “Statins and osteoporosis: new role for old drugs.,” *J. Pharm. Pharmacol.*, vol. 58, pp. 3–18, 2006.

[150] P. Kinra and S. Khan, “Simvastatin: Its potential new role in periodontal regeneration,” *Biol. Med.*, vol. 3, no. (2) Special Issue, pp. 215–221, 2011.

[151] G. E. Gutierrez, D. Lalka, I. R. Garrett, G. Rossini, and G. R. Mundy, “Transdermal application of lovastatin to rats causes profound increases in bone formation and plasma concentrations,” *Osteoporos. Int.*, vol. 17, pp. 1033–1042, 2006.

[152] M. Yamashita, F. Otsuka, T. Mukai, H. Otani, K. Inagaki, T. Miyoshi, J. Goto, M. Yamamura, and H. Makino, “Simvastatin antagonizes tumor necrosis factor-alpha ihibition of bone morphogenetic proteins-2-induced osteoblast differentiation by regulating Smad signaling and Ras/Rho-mitogen-activated protein kinase pathway,” *J. Endocrinol.*, vol. 196, pp. 601–613, 2008.

[153] K. Sakoda, M. Yamamoto, Y. Negishi, J. K. Liao, K. Node, and Y. Izumi, “Simvastatin decreases IL-6 and IL-8 production in epithelial cells.,” *J. Dent. Res.*, vol. 85, pp. 520–523, 2006.

[154] Z. Wu, C. Liu, G. Zang, and H. Sun, “The effect of simvastatin on remodelling of the alveolar bone following tooth extraction.,” *Int. J. Oral Maxillofac. Surg.*, vol. 37, pp. 170–176, Feb. 2008.

[155] I. Ozeç, E. Kiliç, C. Gümüş, and F. Göze, “Effect of local simvastatin application on mandibular defects.,” *J. Craniofac. Surg.*, vol. 18, pp. 546–550, 2007.

[156] M. Nyan, D. Sato, M. Oda, T. Machida, H. Kobayashi, T. Nakamura, and S. Kasugai, “Bone formation with the combination of simvastatin and calcium sulfate in critical-sized rat calvarial defect.,” *J. Pharmacol. Sci.*, vol. 104, pp. 384–386, 2007.

[157] J. B. Park, “The use of simvastatin in bone regeneration,” *Medicina Oral, Patologia Oral y Cirugia Bucal*, vol. 14. 2009.

[158] M. S. Morris, Y. Lee, M. T. Lavin, P. J. Giannini, M. J. Schmid, D. B. Marx, and R. A. Reinhardt, “Injectable simvastatin in periodontal defects and alveolar ridges: pilot studies.,” *J. Periodontol.*, vol. 79, pp. 1465–1473, 2008.

[159] X. Huang, Z. Huang, and W. Li, “Highly efficient release of simvastatin from simvastatin-loaded calcium sulphate scaffolds enhances segmental bone regeneration in rabbits,” *Mol. Med. Rep.*, vol. 9, pp. 2152–2158, 2014.

[160] M. Nyan, D. Sato, H. Kihara, T. Machida, K. Ohya, and S. Kasugai, “Effects of the combination with alpha-tricalcium phosphate and simvastatin on bone regeneration.,” *Clin. Oral Implants Res.*, vol. 20, pp. 280–287, 2009.

[161] a R. Pradeep, N. Priyanka, N. Kalra, S. B. Naik, S. P. Singh, and S. Martande, “Clinical efficacy of subgingivally delivered 1.2-mg simvastatin in the treatment of individuals with class II furcation defects: a randomized controlled clinical trial.,” *J. Periodontol.*, vol. 83, pp. 1472–9, 2012.

[162] A. R. Pradeep and M. S. Thorat, “Clinical effect of subgingivally delivered simvastatin in the treatment of patients with chronic periodontitis: a randomized clinical trial,” *J Periodontol*, vol. 81, pp. 214–222, 2010.

[163] T. Tanigo, R. Takaoka, and Y. Tabata, “Sustained release of water-insoluble simvastatin from biodegradable hydrogel augments bone regeneration,” *J. Control. Release*, vol. 143, pp. 201–206, 2010.

[164] S. D. Nath, S. Son, A. Sadiasa, Y. K. Min, and B. T. Lee, “Preparation and characterization of PLGA microspheres by the electrospraying method for delivering simvastatin for bone regeneration,” *Int. J. Pharm.*, vol. 443, pp. 87–94, 2013.

[165] Y. Ayukawa, E. Yasukawa, Y. Moriyama, Y. Ogino, H. Wada, I. Atsuta, and K. Koyano, “Local application of statin promotes bone repair through the suppression of osteoclasts and the enhancement of osteoblasts at bone-healing sites in rats,” *Oral Surgery, Oral Med. Oral Pathol. Oral Radiol. Endodontology*, vol. 107, pp. 336–342, 2009.

[166] M. Nyan, T. Miyahara, K. Noritake, J. Hao, R. Rodriguez, S. Kuroda, and S. Kasugai, “Molecular and tissue responses in the healing of rat calvarial defects after local application of simvastatin combined with alpha tricalcium phosphate,” *J. Biomed. Mater. Res. - Part B Appl. Biomater.*, vol. 93, pp. 65–73, 2010.

[167] E. Pişkin, I. A. Işoğlu, N. Bölgen, I. Vargel, S. Griffiths, T. Çavuşoğlu, P. Korkusuz, E. Güzel, and S. Cartmell, “In vivo performance of simvastatin-loaded electrospun spiral-wound polycaprolactone scaffolds in reconstruction of cranial bone defects in the rat model,” *J. Biomed. Mater. Res. - Part A*, vol. 90, pp. 1137–1151, 2009.

[168] J. C. Junqueira, M. N. G. Mancini, Y. R. Carvalho, A. L. Anbinder, I. Balducci, and R. F. Rocha, “Effects of simvastatin on bone regeneration in the mandibles of ovariectomized rats and on blood cholesterol levels.,” *J. Oral Sci.*, vol. 44, pp. 117–124, 2002.

[169] N. Maciel-Oliveira, V. Bradaschia-Correa, and V. E. Arana-Chavez, “Early alveolar bone regeneration in rats after topical administration of simvastatin,” *Oral Surgery, Oral Med. Oral Pathol. Oral Radiol. Endodontology*, vol. 112, pp. 170–179, 2011.

[170] C. E. V. C. Lima, J. C. Calixto, and A. L. Anbinder, “Influence of the association between simvastatin and demineralized bovine bone matrix on bone repair in rats,” *Braz Oral Res.*, vol. 25, no. 1, pp. 42–48, 2011.

[171] A. L. Anbinder and J. C. Junqueira, “Influence of Simvastatin on Bone Regeneration of Tibial Defects and Blood Cholesterol Level in Rats,” vol. 17, pp. 267–273, 2006.

[172] L. Ferreira, M. H. Gil, and J. S. Dordick, “Enzymatic synthesis of dextran-containing hydrogels,” *Biomaterials*, vol. 23, no. 19, pp. 3957–3967, 2002.

[173] International Organization for Standardization, “ISO 13779-6:2015(en) Implants for surgery — Hydroxyapatite.” [Online]. Available: https://www.iso.org/obp/ui/#iso:std:iso:13779:-6:ed-1:v1:en. [Accessed: 20-Sep-2014].

[174] J. P. Cassella, N. Garrington, T. C. B. Stamp, and S. Y. Ali, “An electron probe x-ray microanalytical study of bone mineral in osteogenesis imperfecta,” *Calcif. Tissue Int.*, vol. 56, no. 2, pp. 118–122, 1995.

[175] J. V. Lobato, N. S. Hussain, C. M. Botelho, A. C. Maurício, A. Afonso, N. Ali, and J. D. Santos, “Assessment of Bonelike® graft with a resorbable matrix using an animal model,” *Thin Solid Films*, vol. 515, no. 1, pp. 362–367, 2006.

[176] M. A. Lopes, J. D. Santos, F. J. Monteiro, and J. C. Knowles, “Glass-reinforced hydroxyapatite: A comprehensive study of the effect of glass composition on the crystallography of the composite,” *J. Biomed. Mater. Res.*, vol. 39, no. 2, pp. 244–251, 1998.

[177] M. A. Lopes, J. C. Knowles, J. D. Santos, F. J. Monteiro, and I. Olsen, “Direct and indirect effects of P2O5 glass reinforced-hydroxyapatite composites on the growth and function of osteoblast-like cells,” *Biomaterials*, vol. 21, no. 11, pp. 1165–1172, 2000.

[178] M. A. Lopes, J. D. Santos, F. J. Monteiro, C. Ohtsuki, A. Osaka, S. Kaneko, and H. Inoue, “Push-out testing and histological evaluation of glass reinforced hydroxyapatite composites implanted in the tibia of rabbits,” *J. Biomed. Mater. Res.*, vol. 54, no. 4, pp. 463–469, 2001.

[179] F. Duarte, J. D. Santos, and A. Afonso, “Medical applications of Bonelike in Maxillofacial Surgery,” *Mater. Sci. Forum*, vol. 455–456, pp. 370–373, 2004.

[180] X. Z. Zhang, P. Jo Lewis, and C. C. Chu, “Fabrication and characterization of a smart drug delivery system: Microsphere in hydrogel,” *Biomaterials*, vol. 26, no. 16, pp. 3299–3309, 2005.

[181] S. M. Nuño-Donlucas, J. C. Sánchez-Díaz, M. Rabelero, J. Cortés-Ortega, C. C. Luhrs-Olmos, V. V. Fernández-Escamilla, E. Mendizábal, and J. E. Puig, “Microstructured polyacrylamide hydrogels made with hydrophobic nanoparticles,” *J. Colloid Interface Sci.*, vol. 270, no. 1, pp. 94–98, 2004.

[182] L. J. Puig, J. C. Sánchez-Díaz, M. Villacampa, E. Mendizábal, J. E. Puig, a. Aguiar, and I. Katime, “Microstructured Polyacrylamide Hydrogels Prepared Via Inverse Microemulsion Polymerization.,” *J. Colloid Interface Sci.*, vol. 235, no. 2, pp. 278–282, 2001.

[183] S. Dina, N. Cláudia, P. Isabel, M. Ana, D. Maria, C. Manuel, and G. Francisco, “Structural analysis of dextrins and characterization of dextrin-based biomedical hydrogels,” *Carbohydr. Polym.*, vol. 114, no. 2014, pp. 458–466, 2014.

[184] R. Tan, X. Niu, S. Gan, and Q. Feng, “Preparation and characterization of an injectable composite,” *J. Mater. Sci. Mater. Med.*, vol. 20, no. 6, pp. 1245–1253, 2009.

[185] F. Cilurzo, F. Selmin, P. Minghetti, M. Adami, E. Bertoni, S. Lauria, and L. Montanari, “Injectability evaluation: an open issue.,” *AAPS PharmSciTech*, vol. 12, no. 2, pp. 604–609, 2011.

[186] I. Khairoun, F. C. Driessens, M. G. Boltong, J. A. Planell, and R. Wenz, “Addition of cohesion promotors to calcium phosphate cements.,” *Biomaterials*, vol. 20, no. 4, pp. 393–398, 1999.

[187] I. Khairoun, M. G. Boltong, F. C. Driessens, and J. A. Planell, “Some factors controlling the injectability of calcium phosphate bone cements.,” *J. Mater. Sci. Mater. Med.*, vol. 9, no. 8, pp. 425–428, 1998.

[188] M. Bohner and G. Baroud, “Injectability of calcium phosphate pastes,” *Biomaterials*, vol. 26, no. 13, pp. 1553–1563, 2005.

[189] D. Stein, Y. Lee, M. J. Schmid, B. Killpack, M. A. Genrich, N. Narayana, D. B. Marx, D. M. Cullen, and R. A. Reinhardt, “Local simvastatin effects on mandibular bone growth and inflammation.,” *J. Periodontol.*, vol. 76, no. 11, pp. 1861–1870, 2005.

[190] R. W. K. Wong and A. B. M. Rabie, “Statin collagen grafts used to repair defects in the parietal bone of rabbits,” *Br. J. Oral Maxillofac. Surg.*, vol. 41, no. 4, pp. 244–248, 2003.

[191] R. Mulik, K. Mahadik, and A. Paradkar, “Development of curcuminoids loaded poly(butyl) cyanoacrylate nanoparticles: Physicochemical characterization and stability study,” *Eur. J. Pharm. Sci.*, vol. 37, no. 3–4, pp. 395–404, 2009.

[192] C. Gonçalves, P. Pereira, and F. M. Gama, “Self-assembled hydrogel nanoparticles for drug delivery applications,” *Materials (Basel).*, vol. 3, pp. 1420–1460, 2010.